



**NEAR EAST UNIVERSITY  
INSTITUTE OF GRADUATE STUDIES  
DEPARTMENT OF PETROLEUM AND NATURAL GAS  
ENGINEERING**

**NUMERICAL SIMULATION OF CO<sub>2</sub> INJECTION FOR  
EOR IN THE ALWYN FIELD, NORTH SEA, UK**

**M.Sc. THESIS**

**Olisa Leonard OSIMIRI**

**Nicosia  
June, 2022**

**OLISA LEONARD  
OSIMIRI**

**NUMERICAL SIMULATION OF CO<sub>2</sub>  
INJECTION FOR EOR IN THE ALWYN  
FIELD, NORTH SEA, UK**

**MASTER THESIS**

**2022**

**NEAR EAST UNIVERSITY  
INSTITUTE OF GRADUATE STUDIES  
DEPARTMENT OF PETROLEUM AND NATURAL GAS  
ENGINEERING**

**NUMERICAL SIMULATION OF CO<sub>2</sub> INJECTION FOR  
EOR IN THE ALWYN FIELD, NORTH SEA, UK.**

**M.Sc. THESIS**




**Olisa Leonard OSIMIRI**

**Supervisor  
Prof. Dr. Cavit ATALAR**


**Nicosia  
June, 2022**

### Approval

We certify that we have read the thesis submitted by Olisa Leonard OSIMIRI titled “Numerical Simulation of CO<sub>2</sub> Injection for EOR in the Alwyn Field, North Sea, UK.” and that in our combined opinion it is fully adequate, in scope and in quality, as a thesis for the degree of Master of Applied Sciences.

Examining Committee	Name-Surname	Signature
Head of the Committee:	Prof. Dr. Salih SANER	
Committee Member:	Assoc. Prof. Dr. Huseyin CAMUR	
Supervisor:	Prof. Dr. Cavit ATALAR	

Approved by the Head of the Department

29/06/2022  
  
Prof. Dr. Cavit ATALAR  
Head of Department

Approved by the Institute of Graduate Studies

29/06/2022  
  
Prof. Dr. Kemal Hüsnü Can Başer  
Head of the Institute

## **Declaration**

I hereby declare that all information, documents, analysis and results in this thesis have been collected and presented according to the academic rules and ethical guidelines of Institute of Graduate Studies, Near East University. I also declare that as required by these rules and conduct, I have fully cited and referenced information and data that are not original to this study.

Olisa Leonard OSIMIRI

29/06/2022

## **Acknowledgement**

Firstly, I would like to thank my supervisor Prof. Dr. Cavit Atalar for his endless support and guidance throughout this project and Miss Palang Moronke Guful for her assistance and guidance in making sure this research was a success. Also I would like to appreciate Prof. Dr. Salih Saner, Assoc. Prof. Dr. Huseyin Camur and the entire staff of our able department for their tremendous support. Secondly, to my immediate family; my mum Ngozi, my step dad, Ignatius Anopuo and my Uncle Dr. Thaddeus Eze, for their financial support and encouragement in my academic pursuit. To my siblings; Chika, Chinwe, Amarachi and Tobeche Eze I want to say I appreciate all your love and care towards me. Thirdly, to my friends Mr Azubuike Hope Amadi, Miss Helen Sunday and all my well-wishers too numerous to mention, I want to appreciate you all for being my friends and making this work a success. Words cannot express how grateful I am to you all, since actions they say, speak louder than words, the best I can do to show my appreciation is to put in my best in my academic pursuit

Lastly, I would want to thank Microsoft for developing such a wonderful tool like MS Word and MS Excel. They made the typing of my work easier.

**Olisa Leonard OSIMIRI**

## Abstract

### Numerical Simulation and Analysis of CO<sub>2</sub> Injection for EOR in the Alwyn

Field, North Sea, UK.

OSIMIRI, Leonard Olisa

MSc. Department of Petroleum and Natural Gas Engineering

June, 2022, 105 pages

As increased extraction of oil is shifting from primary and secondary recovery, it is expected to employ enhanced oil recovery techniques. When compared to the numerous gases used during area sweeping during the optimization of oil production, CO<sub>2</sub> has the unique capacity to chemically dissolve in reservoir oil due to its flow property and viscosity, and vaporise lighter ends of hydrocarbon from reservoir oil. In this study, the numerical reservoir Eclipse simulator was used to analyse the performance of miscible CO<sub>2</sub> injection compared to natural depletion and immiscible gas flooding in the Alwyn field.

During the scenario of natural depletion, the reservoir pressure decreased quickly and steadily. This behaviour of the pressure in the reservoir is related to the lack of gas caps or extraneous fluids that may replace the gas and oil withdrawals. The field was produced for 3.6 years before reaching its economic limit of 1000 sm<sup>3</sup>/day of oil. Field gas-oil ratio (FGOR) was 1500 Sm<sup>3</sup>/Sm<sup>3</sup> it increased rapidly with a reduction in pressure below the bubble point (258.2 bars), as field watercut (FWCT) increased to 67%.

The gas injection scenario, there was less water production as field water cut was about 56% after 6years of production. At pressures beyond saturation pressure, there was an early gas breakthrough, and the gas-oil ratio steadily increased. Compared to natural depletion, oil recovery via gas injection has a significantly higher recovery efficiency. The field was produced for about 6.5 years before shut-down. Oil recovery was 32%.

Miscible CO<sub>2</sub> injection had the best production profile and highest oil recovery of about 42%, topping all other simulation scenarios. This is a stepwise decline in pressure due to simultaneous gas and water injection-assisted production. Oil production was sustained for about 9 years before reaching the economic constrain of 1000 sm<sup>3</sup>/d. FWCT increased up to 68%.

**Keywords:** Reservoir simulation, natural depletion, immiscible CO<sub>2</sub> injection, miscible CO<sub>2</sub> injection, Eclipse 100.

## Ozet

### Alwyn Field, Kuzey Denizi, Birleşik Krallık'ta EOR için CO<sub>2</sub> Enjeksiyonunun

#### Sayısal Simülasyonu ve Analizi.

OSIMIRI, Leonard Olisa

yüksek lisans Petrol ve Doğal Gaz Mühendisliği Bölümü

Haziran, 2022, 105 sayfa

Artan petrol ekstraksiyonu, birincil ve ikincil geri kazanımdan kaydığı için, gelişmiş petrol geri kazanım tekniklerinin kullanılması beklenmektedir. Petrol üretiminin optimizasyonu sırasında alan süpürme sırasında kullanılan çok sayıda gazla karşılaştırıldığında, CO<sub>2</sub>, akış özelliği ve viskozitesi nedeniyle rezervuar yağında kimyasal olarak çözünme ve rezervuar yağından hidrokarbonun daha hafif uçlarını buharlaştırma konusunda benzersiz bir kapasiteye sahiptir. Bu çalışmada, Alwyn sahasında doğal tükenme ve karışmayan gaz taşkınlarına kıyasla karışabilir CO<sub>2</sub> enjeksiyonunun performansını analiz etmek için sayısal rezervuar Eclipse simülatörü kullanılmıştır.

Doğal tükenme senaryosu sırasında, rezervuar basıncı hızlı ve istikrarlı bir şekilde azaldı. Rezervuardaki basıncın bu davranışı, gaz ve petrol çıkışlarının yerini alabilecek gaz kapaklarının veya yabancı sıvıların eksikliği ile ilgilidir. Saha, ekonomik limit olan 1000 sm<sup>3</sup>/gün petrole ulaşmadan önce 3.6 yıl boyunca üretildi. Saha gaz-yağ oranı (FGOR) 1500 Sm<sup>3</sup>/Sm<sup>3</sup> idi, basınçta kabarcıklanma noktasının (258,2 bar) altında bir azalma ile hızla arttı, dosyalanmış su kesimi (FWCT) %67'ye yükseldi.

Gaz enjeksiyon senaryosunda, 6 yıllık üretimden sonra saha su kesintisi yaklaşık %56 olduğu için daha az su üretimi olmuştur. Doyma basıncının ötesindeki basınçlarda, erken bir gaz atılımı oldu ve gaz-yağ oranı istikrarlı bir şekilde arttı. Doğal tükenme ile karşılaştırıldığında, gaz enjeksiyonu yoluyla petrol geri kazanımı, önemli ölçüde daha yüksek bir geri kazanım verimliliğine sahiptir. Saha, kapatılmadan önce yaklaşık 6.5 yıl üretildi. Petrol geri kazanımı %32 idi.

Karışabilir CO<sub>2</sub> enjeksiyonu, en iyi üretim profiline ve yaklaşık %42'lik en yüksek petrol geri kazanımına sahipti ve diğer tüm simülasyon senaryolarını geride bıraktı. Bu, eşzamanlı gaz ve su enjeksiyon destekli üretim nedeniyle basınçta kademeli bir düşüştür. Petrol üretimi, 1000 sm<sup>3</sup>/d'lik ekonomik kısıtlamaya ulaşmadan önce yaklaşık 9 yıl sürdürüldü. FWCT %68'e kadar arttı.

**Anahtar Kelimeler:** Rezervuar simülasyonu, doğal tükenme, karışmaz CO<sub>2</sub> enjeksiyonu, karışabilir CO<sub>2</sub> enjeksiyonu, tutulma 100.

## Table of Contents

Approval .....	2
Declaration .....	3
Acknowledgement .....	4
Abstract .....	5
Ozet .....	6
Table of Contents .....	7
List of Tables .....	10
List of Figures .....	11
List of Abbreviations .....	13

### CHAPTER I

Introduction .....	15
Background to the Study .....	15
Statement of the Problem .....	17
Hypothesis .....	17
Aim and Objectives of the Study .....	17
Significance of the Study .....	18
Scope of the Study .....	18
Structure of Thesis .....	18
Limitation of Study .....	18

### CHAPTER II

Literature Review .....	20
Overview of CO <sub>2</sub> -Enhance Oil Recovery .....	20
Fundamentals of CO <sub>2</sub> -EOR .....	20
Miscible CO <sub>2</sub> Displacement Method .....	22
Immiscible CO <sub>2</sub> Displacement Method .....	25
Comparision of Immiscible and Miscible Displacement processes .....	27
CO <sub>2</sub> Solubility in Simulated Live and Dead Oil .....	28
Records of CO <sub>2</sub> for EOR Projects .....	32
Lessons from Miscible CO <sub>2</sub> -EOR Operations .....	33
Lessons Learned from Immiscible CO <sub>2</sub> -EOR Operations .....	35
Implementation Challenges for CO <sub>2</sub> -EOR .....	36



CO <sub>2</sub> -Reservoir Interactions .....	36
Influence on Project Effectiveness .....	36
Impact on Oil Quality.....	36
Infrastructure Processes for CO <sub>2</sub> Capture, Cost Implication and Application .....	37

### CHAPTER III

Methodology .....	40
Reservoir Description.....	40
Reservoir Model Characteristics .....	41
Reservoir Simulation.....	42
Miscible Injection Modeling .....	42
The Todd and Longstaff Mixing Parameter Model .....	42
Model Assumptions and Constraints .....	45
Case 1: Natural Depletion .....	46
Case 2: Immiscible Gas Injection.....	46
Case 3: Miscible CO <sub>2</sub> Injection.....	46
PVT Data.....	46

### CHAPTER IV

Results and Discussion .....	48
Findings.....	48
Natural Depletion .....	49
Immiscible Gas Injection Development Scheme .....	53
Miscible Gas (CO <sub>2</sub> ) Injection.....	56
Comparative Plots .....	61
CO <sub>2</sub> Flooding Projects and Case Studies .....	63

### CHAPTER V

Conclusions and Recommendations .....	67
Conclusions .....	67
Recommendations .....	68
References.....	69
Appendices.....	76
Appendix A: Gas Injection PVT File.....	76

Appendix B: Gas Injection Simulation File .....	85
Appendix C: Turnitin Similarity Report .....	103
Appendix D: Ethical Approval Letter.....	104

## List of Tables

<b>Table 2.1.</b> Comparison between miscible and immiscible displacement CO <sub>2</sub> -EOR techniques	27
<b>Table 3.1.</b> Parameters used for reservoir simulation on the alwyn field	47
<b>Table 4.1.</b> Position and grid geometry of wells for natural depletion	50
<b>Table 4.2.</b> Position and grid geometry of wells for gas injection	54
<b>Table 4.3.</b> Position and grid geometry of wells for miscible CO <sub>2</sub> injection	58
<b>Table 4.4.</b> Summary of simulation results of natural depletion, gas injection and miscible CO <sub>2</sub> injection	62
<b>Table 4.5.</b> CO <sub>2</sub> miscible flooding operator and production dataset	64
<b>Table 4.6.</b> Properties of reservoirs subjected to CO <sub>2</sub> flooding dataset	65

## List of Figures

<b>Figure 2.1.</b> A stable front pattern of CO <sub>2</sub> injection and the oil (a) and viscous fingering (b)	21
<b>Figure 2.2.</b> WAG patterns	22
<b>Figure 2.3.</b> Early CO <sub>2</sub> breakthrough as a result of non-optimal gravity factor and viscous flow	24
<b>Figure 2.4.</b> A schematic of the immiscible displacement technique	26
<b>Figure 3.1.</b> Alwyn field localization map	40
<b>Figure 3.2.</b> Brent geological cross section	41
<b>Figure 4.1.</b> Faults in the alwyn field (non-transmissible fault in yellow, transmissible in green)	48
<b>Figure 4.2.</b> Well position for initial development scenario	49
<b>Figure 4.3.</b> Well position for gas natural depletion scenario	50
<b>Figure 4.4.</b> Depletion of field after producing with natural depletion injection	51
<b>Figure 4.5.</b> Poor oil production from well Y2 (later converted to a gas injector)	51
<b>Figure 4.6.</b> Plot of FOPR, FGOR, FWCT, and FPR for natural depletion	52
<b>Figure 4.7.</b> Well position for gas injection scenario	53
<b>Figure 4.8.</b> Depletion of field after producing with gas injection	54
<b>Figure 4.9.</b> Field gas injection profile for gas injection scenario	55
<b>Figure 4.10.</b> Gas injection wells plot (Y2 shows more potential contribution as an injector)	55
<b>Figure 4.11.</b> Field performance plots for gas injection scenario	56
<b>Figure 4.12.</b> Some miscibility functionalities used for miscible flooding	57
<b>Figure 4.13.</b> Well position for miscible flooding scenario	58
<b>Figure 4.14.</b> Depletion of field after producing with miscible flooding	59
<b>Figure 4.15.</b> Field performance plots for miscible flooding scenario	60
<b>Figure 4.16.</b> Field injection plots for miscible flooding scenario	60
<b>Figure 4.17.</b> Field oil production performance plots for initial, natural depletion, immiscible gas injection and miscible flooding development scenario	61
<b>Figure 4.18.</b> Field water cut plots for initial, natural depletion, immiscible gas Injection and miscible flooding development scenario	62
<b>Figure 4.19.</b> Field water and gas injection in relation to field pressure during	

miscible flooding in comparison to field pressure during initial, natural,  
and gas injection 63

**Figure 4.20.** Comparison of oil recoveries using CO<sub>2</sub> in EORs with Alwyn case study 66

### List of Abbreviations

<b>AI:</b>	Artificial Intelligence
<b>BCU:</b>	Base Cretaceous Unconformity
<b>BR:</b>	Bayesian Regularization
<b>CCU:</b>	Carbon Capture and Utilization
<b>CCS:</b>	Carbon Capture Sequestration
<b>DE:</b>	Differential Evolution
<b>EOR:</b>	Enhanced Oil Recovery
<b>EU:</b>	European Union
<b>EUR</b>	Expected Ultimate Recovery
<b>FGIR:</b>	Field Gas Injection Rate
<b>FGOR:</b>	Field Gas Oil Ratio
<b>FOE:</b>	Field Oil Efficiency
<b>FOPR:</b>	Field Oil Production Rate
<b>FPR:</b>	Field Pressure Rate
<b>FPSO:</b>	Floating Production Storage and Offtake
<b>FWCT:</b>	Field Water Cut
<b>FWIR:</b>	Field Water Injection Rate
<b>GA:</b>	Genetic Algorithm
<b>GEP</b>	Gene Expression Programme
<b>GHG:</b>	Green House Gas
<b>GMDH:</b>	Group Method of Data Handling
<b>GSGI:</b>	Gravity Stable Gas Injection
<b>IFT:</b>	Interfacial Tension
<b>IGCC:</b>	Integrated Gasification Combined Cycle
<b>LM:</b>	Levenberg-Marquardt
<b>LSSVM:</b>	Least Square Support Vector Machine
<b>MCM:</b>	Multiple Contact Miscibility
<b>MMP:</b>	Minimum Miscibility Pressure
<b>MW:</b>	Molecular Weight
<b>OOIP:</b>	original oil in place
<b>Ps:</b>	Saturation Pressure
<b>PVT:</b>	Pressure Volume Temperature

<b>RB:</b>	Resilient Backpropagation
<b>RBF</b>	Radial Basis Function
<b>Rs:</b>	Solution Gas-Oil Ratio
<b>SCG:</b>	Scaled Conjugate Gradient
<b>SF:</b>	Swelling Factor
<b>T:</b>	Temperature
<b>Tc:</b>	Critical Temperature
<b>UKCS:</b>	United Kingdom Continental Shelf
<b>UOP:</b>	Universal Oil Products
<b>WAG:</b>	Water Alternating Gas
<b>WIGR:</b>	Well Gas Injection Rate

## CHAPTER I

### Introduction

#### Background to the Study

Globally, the production of crude oil and natural gas from reserves have been of great benefit to numerous areas of the world economy serving as a raw material source and primary energy for the industrial advancements of many countries. Speculations are that the demand is expected to increase exponentially over the next five decades as countries around the world further industrialize and population continues to increase at unprecedented rates. Therefore, it is essential to know the number of oil reserves that are proven reserves (more than 90% likelihood of being able to extract the oil), probable reserves (more than 50% likelihood of being able to extract the oil), and possible reserves (less than 50% chances of extracting the oil) (Ranathunga et al., 2014).

The knowledge of this information will help in determining the capacity of the future supply and where its supply will come from. According to research carried in 2016 by Worldometer, the world oil reserves was estimated to be 1,650,585,140,000 barrels and the consumption value was 35,442,913,090 barrels per year turning out that 97,103,871 barrels are consumed per day (Worldometers, 2022). From this estimation, it can be said there is still oil in reserve. However, getting to extract this oil from reserves is not as straightforward as it used to be because many oil reservoirs in recent times around the world have started indicating a decline in production and may not be able to cater for the world's demands.

Oilfields has some factors that needs to be understood to know the depletion pattern of the reservoir. Basically, the recovery of oil in oilfields is through fluid flows in porous material. Therefore, the constitutes of the fluid present and the geological makeup properties of the reservoir has a lot to do with the extraction of oil. The difference makes fields not to be uniform all over in term of production rate. Pore spaces serves as bearers of oil in reservoir, and the term porosity means pore volume fraction to the total bulk volume. So, the more the porosity, the better the storing capacity of the rock (Ranathunga et al., 2014). For fluid flows, the pores serve as a network of storage and transfer.



The production of oil is generally carried out in three stages: primary, secondary, and tertiary. Primary oil recovery for oil production solely depends on the natural drive of the reservoir which is the difference in pressure without external aid between the production well pressure and the reservoir pressure. When the rate of production is getting slow and the reservoir can't push the oil to surface effectively then, the second stage of oil production is employed.

Secondary oil recovery is usually done by pumping of fluid (usually H<sub>2</sub>O) into the reservoir to serve as an artificial drive aiding the increase of the reservoir pressure. Primary and secondary oil production mechanism only enables a recovery efficiency of about 33 percent of the total amount of oil present in the reservoir, which is also known as the original oil in place (OOIP). However, to further increase the amount of oil recovery usually towards the declining phase of the reservoir, enhanced oil recovery mechanism is used.

Enhanced or tertiary oil recovery can be achieved by different techniques. They are; chemical injection, gas injection, microbial injection, thermal recovery or ultrasonic stimulation which are explained in details (Lake et al., 2015). According to the research of Green & Willhite (2018) on the movement of chemical species in the displacement oil during chemical injection process, it is not economically feasible to carry out a continuous injection of chemicals.

Nonetheless, with the injection of CO<sub>2</sub> into the oil reservoir, the oil mobility increases which enhances oil production. This is because injecting CO<sub>2</sub> draws out heavy hydrocarbons from the oil phase and speeds up the oil mobility by oil swelling and reducing oil viscosity (Tunio et al., 2011). Therefore, enhanced oil recovery through CO<sub>2</sub> injection in reservoirs remarkably increases oil production. In this modern world of the oil and gas industry, injection of CO<sub>2</sub> for enhanced oil recovery is known as the second largest enhanced oil recovery process in the world, following the thermal operations employed in heavy oil fields (Kulkarni, 2018).

Global warming which is due to the increasing amount of CO<sub>2</sub> and other greenhouse gases like methane, nitrogen oxide in the atmosphere have caused a spontaneous increase in the sea levels and sporadic changes in climate (Schrag, 2017).

The question now is, could squeezing out oil from reservoir save our environment or reduce global warming? Yes, the utilization of carbon from carbon capture as feedstock in the chemical industry creates a chained of curbing pollution

of the environment. However, enhanced oil recovery (EOR) gives the highest industrial use of it. For this mechanism roughly 7 to 23% recovery has been recorded possible globally. The main benefits of CO<sub>2</sub> injection over alternative sources of gases are its cost saving, wide availability, and ease of achieving miscibility condition (Rentar, 2018).

### **Statement of the Problem**

The need for energy is rising daily along with the population. As a result of the ongoing need for oil recovery brought on by the emergence of new markets, the oil and gas industry has been forced to revisit low-pressure oil fields in an effort to recover oil that has become trapped in the pores of the reservoir rock. As the climate continues to change, CO<sub>2</sub>, one of the greenhouse gases, has also contributed to sea level rise and ecosystem imbalance (Perera et al., 2017). Consequently, it is necessary to supply the need for energy while also protecting the environment. In order to meet this, it is recommended that this method of CO<sub>2</sub> injection for oil recovery be researched.

### **Hypothesis**

In order to achieve the aim and objectives of this study, the following hypothesis were made;

- CO<sub>2</sub> injection as an EOR technique can improve the oil production rate
- Production performance differences differ on different drive mechanisms
- Injection fluid miscibility plays a role in improving oil production efficiency

### **Aim and Objectives of the Study**

The aim of this study is to give a numerical simulation and comparison of natural depletion, immiscible and miscible CO<sub>2</sub> injection for enhanced oil recovery. To achieve this aim, the objectives of the study are to:

- Provide a comprehensive study and review of the carbon dioxide enhanced oil recovery process.
- Compare this technique with other enhanced oil recovery techniques
- Generate a numerical simulation using eclipse for its process on a reservoir.

## **Significance of the Study**

The concern of controlling environmental pollution of CO<sub>2</sub> emission is part of the global effort of having a balance and sustainable ecosystem. Undoubtedly, the use CO<sub>2</sub> has helped to a great extent to achieve this aside its application in recovery of oil from reservoirs which the world needs to meet its energy demand. This study therefore is significant in adding to the research work done in understanding the peculiarity of CO<sub>2</sub> injection for enhanced oil recovery.

## **Scope of the Study**

For the purpose of this study, we would be looking at the fundamentals of CO<sub>2</sub> injection process in both miscible and immiscible modes, comprehensive explanation of how CO<sub>2</sub> enhanced oil recovery process could be facilitated in practice, also the laboratory tests involved will be discussed and lastly a numerical simulation to depict production from an oil reservoir will be done using Eclipse from validated acquired data.

## **Structure of Thesis**

The first chapter discusses the topic and its logic, as well as the issues, scope, and constraints. This overview is intended to keep the reader interested in the literature that assisted the researcher in the best approach for achieving the study's goals. This led to chapter two, where many studies relevant to enhanced oil recovery were highlighted, their merits and flaws were evaluated, and the literature reviews indicated the gap in literature that this study filled. The resources and procedures used to achieve the study's goals were outlined in the third chapter. The findings were reported in chapter four based on the methods used, and the results were critically analysed. The study's general conclusion is presented in chapter five, along with recommendations for future research in this field.

## **Limitation of Study**

Although this study is a black oil analysis because it took into account the miscibility of injection fluid with reservoir fluid, an ideal replication of what happens in the field is contingent on the data's accuracy. As a result, the precision of the data utilized to replicate the use of EOR on Alwyn field is limited to the accuracy during data collection. To avoid sabotage and protect company secrets, oil corporations have

historically protected their data. As a result, due to the difficulty of gathering data from other similar fields for comparison, this study's research of the effectiveness of CO<sub>2</sub> for flooding utilizing eclipse simulator was limited to Alwyn field.

## CHAPTER II

### Literature Review

#### Overview of CO<sub>2</sub>-Enhance Oil Recovery

Primary oil recovery, secondary oil recovery, and enhanced oil recovery (EOR) are the three main phases of oil production technology (European Commission, 2005). Primary and secondary oil recovery gives estimated recovery of 33% of original oil in place (OOIP) (Peteves, 2018). EOR techniques were developed in three categories to recover a considerable amount of the remaining OOIP in reservoirs: solvent, chemical, and thermal EOR (Gozalpour, 2015). According to Tzimas et al. (2015), the overall number of EOR projects initially fell before gradually increasing. In 2002 and 2005, utilization of gas for EOR was recorded to be more than thermal EOR. The world today has CO<sub>2</sub> as the most utilized injection gas for recovery among other gases. This is due to its availability and affordability. In the US, it is regarded as the ideal option for increasing oil production.

The availability of CO<sub>2</sub> sources is the first step in a typical CO<sub>2</sub>-EOR project screening. From its industrial or natural source, it can be transferred via pipeline into an injection well. While nearby, tandem system are at times employed instead. The CO<sub>2</sub> recycling plant isolates the CO<sub>2</sub> produced and injects it back into the system to boost oil production. Furthermore, the injected CO<sub>2</sub> may be able to be stored in a geological reserve. Oil reservoirs are thus regarded as ideal geological media for CO<sub>2</sub> storage in this fashion. Because CO<sub>2</sub> is one of the greenhouse gases, an EOR project using industrial CO<sub>2</sub> sources reduces anthropogenic CO<sub>2</sub> emissions from human activities, that has a positive influence on climate change greenhouse gas (GHG) (European Commission, 2005). The integration of using CO<sub>2</sub> for oil recovery and carbon capture and storage (CCS) has provided the world with energy and environmental benefits (European Commission, 2005, 2017, 2018). A researched and modelled numerical simulation and analysis of CO<sub>2</sub> injection for enhanced oil recovery: a case study, considering the potential of CO<sub>2</sub>- EOR technology.

#### Fundamentals of CO<sub>2</sub>-EOR

The oil deposit in the reservoir after the secondary recovery mechanism still has more than 50% of the initial oil content in the reservoir. The left-over oil are

trapped in the rock pores of the reservoir. However, during primary and secondary recovery approximately 20 – 35% of the oil is swept by the displacing fluids. Meaning greater amount of more than 50% is still present in the reservoir (Georgakaki, 2005).

Therefore, there is need to recover this large portion of the oil by considering its entrapment in the pores. The method of CO<sub>2</sub> injection can mobilize this entrapped oil. When injected, it interacts with the contained oil and reservoir rock chemically and physically, making possible conditions to recover the oil, which are; volume expansion of oil by reducing its viscosity, capillary forces reduction to minimise interfacial tension between the reservoir rock and oil, forming of conducive phase changes to increase fluidity in the oil, improvement of the volume sweep efficiency (Georgakaki, 2005).

The applicability of CO<sub>2</sub>-EOR is possible under two processes; miscible displacement and immiscible displacement depending on the condition of the reservoir. Also, it can be carried out base on mechanism of injection; (1) the gravity stable gas injection (GSGI) and (2) the water alternating gas (WAG) ( Tzimas, 2015; Georgakaki, 2005).

Figure 2.1, depicts a flow diagram of the process. Furthermore, the movement of CO<sub>2</sub> into the trapped pores of the oil is ease quickly by the water. Depending on the reservoir conditions, different WAG injection patterns are utilized. However, there are variation between the amount of CO<sub>2</sub> injected before and after the water which creates the patterns in figure 2.2.

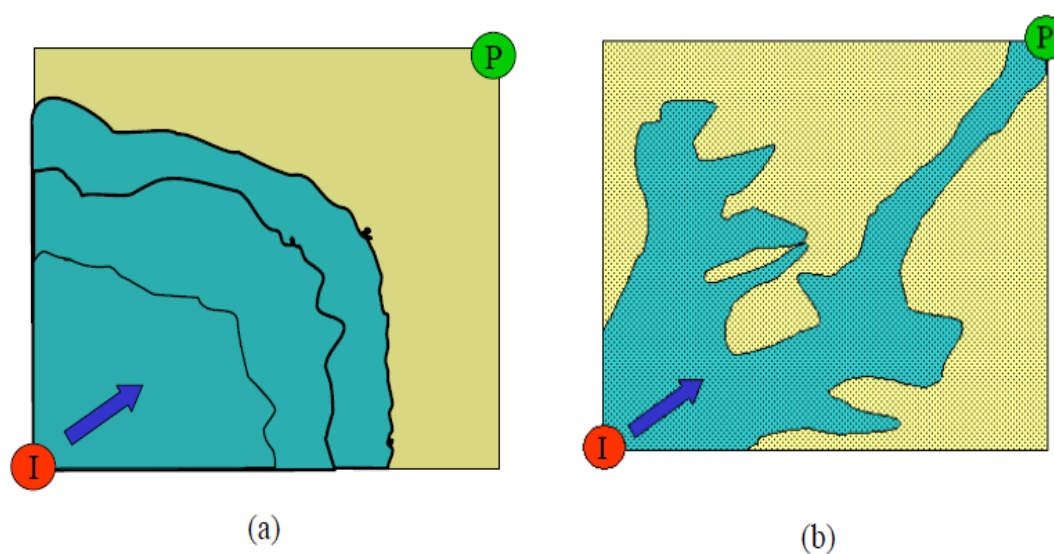


Figure 2.1. A *Stable Front Pattern of CO<sub>2</sub> Injection and the Oil (a) and Viscous Fingering (b)* (Conaway & Pennwell, 2008)

Large portion of the reservoir that is not affected during CO<sub>2</sub> injection creates viscous fingering as shown above; Injection (I) and Production (P) (Conaway and Pennwell, 2008).

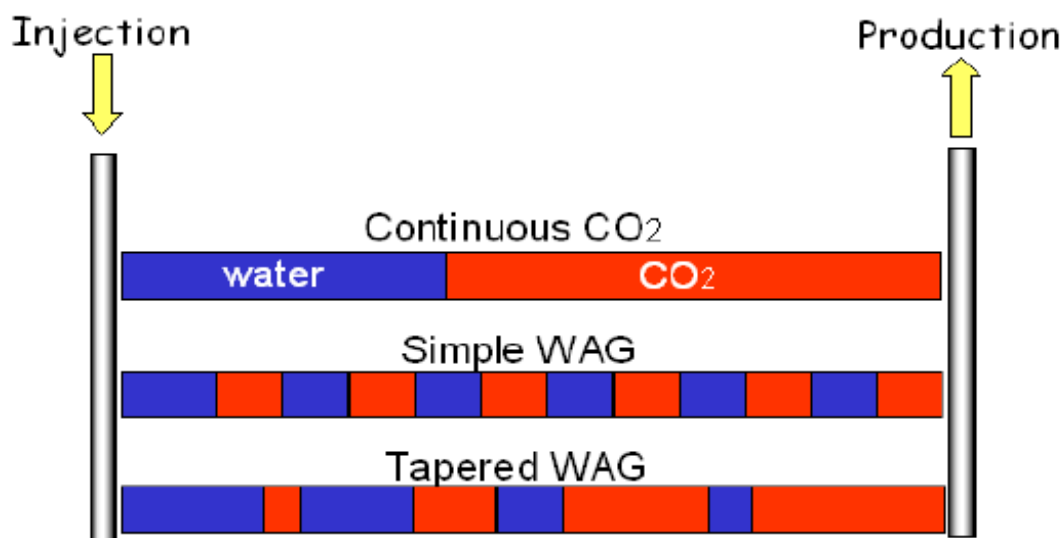


Figure 2.2. WAG Patterns (Pierce, 2017)

Another way of injecting CO<sub>2</sub> is through the crest, causing the oil to be flushed down to the rim where we have the production well, a technique known as gravity stable gas injection (GSGI). CO<sub>2</sub> is used to maintain reservoir pressure and stabilize displacements for high sweep. WAG is of the advantage of having it possible on a small scale, whereas GSGI is typically used across the entire oilfield. As a result, GSGI yield more recovery of oil and CO<sub>2</sub> storage (Goodwear, 2017).

### Miscible CO<sub>2</sub> Displacement Method

Supercritical CO<sub>2</sub> can become miscible with petroleum under favourable reservoir pressure and temperature circumstances, as well as crude oil composition, generating a single-phase liquid. This increases the oil swell volume, and decreases both its surface tension and viscosity to enhance fluidity of the oil out of the reservoir. Carbon dioxide, on the other hand, is not instantly miscible with oil when it comes into contact with it. Multiple contact miscibility is experienced in the reservoir when the CO<sub>2</sub> interact with the oil in the reservoir creating compositional changes. When CO<sub>2</sub> is introduced into a reservoir and comes into touch with crude, is first enhanced with oil intermediates that have been evaporated. The miscibility of oil and CO<sub>2</sub>

(vaporizing process) is enabled by this local change in oil composition. However, in practice, the interaction between CO<sub>2</sub> and oil is more complicated, including the development of several complex liquids and vapour phases (Green and Willhite, 2018).

Figure 2.1; the complete sweep of the reservoir is ensured by a steady shape between the injected CO<sub>2</sub> and the oil (left). The breakthrough of CO<sub>2</sub> occurs due to viscous fingering (right), leaving extensive areas of the reservoir undisturbed by CO<sub>2</sub> injection (Conaway & Pennwell, 2008). Pressure has a significant impact on CO<sub>2</sub> miscibility in crude oil. To make CO<sub>2</sub> entirely miscible with oil, a MMP is required. CO<sub>2</sub> has a density that is similar to crude oil at that pressure.

The value of MMP is determined by the crude oil composition, CO<sub>2</sub> purity, and reservoir conditions (pressure and temperature). As a result, a miscible CO<sub>2</sub>-displacement approach can only be applicable at higher pressure than MMP but lesser reservoir pressure. These circumstances are most commonly seen in the North Sea's oil reservoirs, which are found at depths more than 700 meters. As a result, understanding minimum miscible pressure (MMP) is a prerequisite for determining the process's suitability in an oilfield. To this purpose, a lot of studies have been done on measuring and predicting MMP levels. Using empirical formulae and thermodynamic models, the MMP may currently be quantify experimentally or predicted with great accuracy. Green and Willhite (2018) present a review of current understanding on the subject. In summary, low MMP values, which are required for the procedure to apply to a vast number of oilfields, are favoured by:

- To achieve miscibility in pentane(C5) to botryococcene (C30) hydrocarbons of crude oil, high CO<sub>2</sub> concentrations, such as 0.4-0.75 g/cm<sup>3</sup>, are necessary (DTI SHARP, 2019).
- To maximize CO<sub>2</sub> density, keep reservoir temperatures low.
- High CO<sub>2</sub> purity, as MMP is increased by the presence of contaminants such as nitrogen, sulfur, and others in the CO<sub>2</sub> stream (Technology, 2018).
- Low percentages of aromatics which are lighter than 21°API oil.

The purity of CO<sub>2</sub> recovered from combustion facilities for use in EOR is significantly impacted by this. The MMP varies between 18 and 25 MPa for light, low-S8 North Sea crude oils (DTI SHARP, 2019). Theoretically, oil that has been exposed to CO<sub>2</sub> can be obtained. In practice, however, further oil recovery is usually



limited to 5-20% of OOIP (Goodwear, 2017). Oil recovery is hampered by several factors, including:

- Before full miscibility is attained, CO<sub>2</sub> must flow through the reservoir for a finite distance.
- Free flow of CO<sub>2</sub> causes viscous fingering than oil in the reservoir causing oil entrapment (Figure 2.1).
- Phase segregation is the result of early CO<sub>2</sub> breakthrough caused by unstable movement due to gravity effects (Figure 2.3).
- The need for CO<sub>2</sub> to mobilize some of the water in the reservoir left over from floods.

In order to lessen the likelihood of unstable flow and the amount of CO<sub>2</sub> needed for the operation, CO<sub>2</sub> and water are frequently injected into the reservoir in the WAG manner mentioned above. Compared to CO<sub>2</sub>, water moves through the reservoir more consistently and effectively.

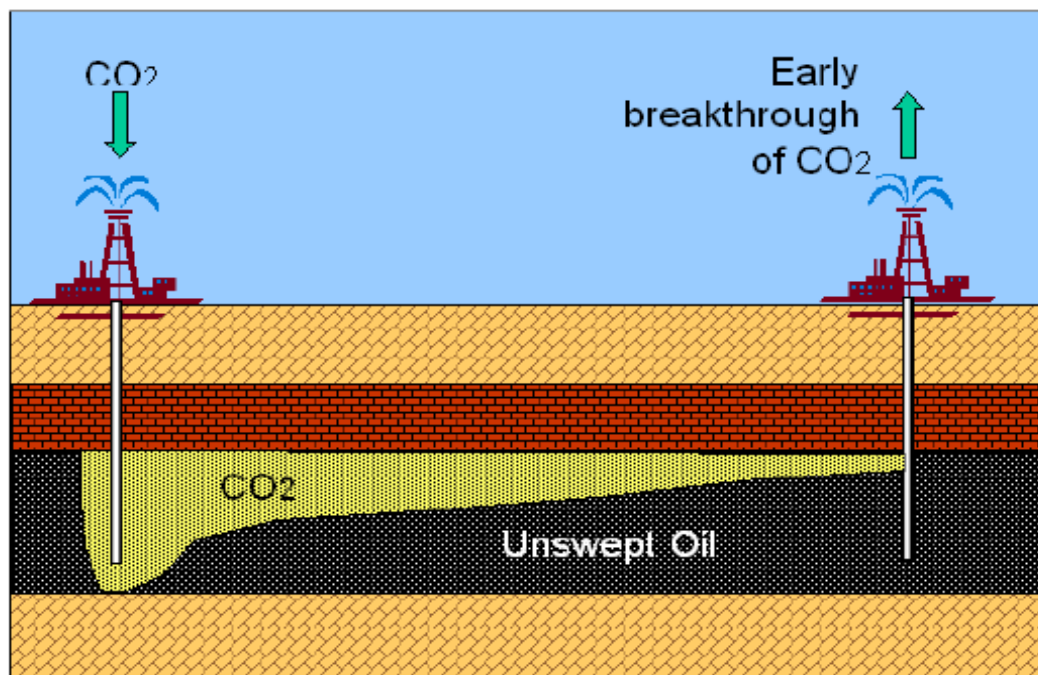


Figure 2.3. *Early CO<sub>2</sub> Breakthrough as a Result of Non-Optimal Gravity Factor and Viscous Flow (Gozalpour, 2015)*

Oil firms frequently aim to reduce CO<sub>2</sub> emissions while increasing oil recovery; recovering CO<sub>2</sub> that leaks from producing wells will appear more cost

effective than purchasing fresh CO<sub>2</sub>, CO<sub>2</sub> is a commodity that might be used for EOR. The acquisition and pre-treatment of CO<sub>2</sub> before injection typically account for half to eighty percent of the operating costs in ongoing CO<sub>2</sub>-EOR projects (Schulte, 2014; Gozalpour, 2015; IEA Greenhouse Gas, 2020). As a result of this, the producing wells are the primary target of most CO<sub>2</sub> injections in miscible operations. Separated from the oil, compressed again, and injected back into the reservoir, the CO<sub>2</sub> that departs from the reservoir joins the flow of new CO<sub>2</sub> brought in for the project. Nonetheless, some CO<sub>2</sub> is permanently buried underground after becoming trapped in reservoir rock pores or getting dissolved in water and oil. According to data from the Ranglely Weber Project in the United States, three parts of CO<sub>2</sub> are re-circulated and ten percent is released into the environment for each CO<sub>2</sub> molecule held in the oil reservoir (IEA Greenhouse Gas, 2020). It is crucial to remember, however, that if keeping CO<sub>2</sub> underground provides financial benefits, to optimise CO<sub>2</sub> retention underground and oil recovery, CO<sub>2</sub> injection may need to be adjusted. According to ongoing research, field-specific optimization will be required, needing an exchange between CO<sub>2</sub> sequestration and oil recovery (Jayasekera, 2015).

Miscible displacement onshore is a commercially viable technology. Because no adjustments to the well pattern are required, operations can be employed at the end of a reservoir's life, a few years before, perhaps even at the very end of secondary oil recovery. The same wells can be used for both miscible and water flooding projects. Additionally, small-scale activities might be carried out in certain reservoir locations. Depending on the reservoir's properties and the distance between the producing and injection wells oil increase can be achieved from the reservoir. To implement an oil recovery operation's miscible displacement project, the following infrastructure is required:

- Facilities for receiving, conditioning and separating CO<sub>2</sub>,
- Modified production and injection wells
- Lines for CO<sub>2</sub> compression and reuse

### **Immiscible CO<sub>2</sub> Displacement Method**

Even when MMP is not attained, such as in low-pressure oil reservoirs or with heavy oils, injecting CO<sub>2</sub> into a reservoir can boost oil recovery. Even while CO<sub>2</sub> is not completely miscible with oil, it can nonetheless partially dissolve in it, causing

swelling. The addition of CO<sub>2</sub> to low-quality heavy oil has been shown to reduce viscosity by a factor of ten (SHARP, 2017). More crucially, CO<sub>2</sub> plays a similar role in immiscible displacement as water does in secondary oil recovery processes, namely, raising and maintaining reservoir pressure.

Although flooding with water has a higher recovery efficiency, using CO<sub>2</sub> to increase reservoir pressure has only been explored in a few number of projects where the reservoir rock's permeability is too low or there are geological reasons why water cannot be used. CO<sub>2</sub> is commonly injected in GSGI mode in this process, but WAG is also an option. CO<sub>2</sub> is usually injected slowly at the reservoir's crest, to fill the reservoir rock's pore volume. An artificial gas cap is created by the gas injection, and oil is pushed down and toward the reservoir's rim, where the producing wells are located.

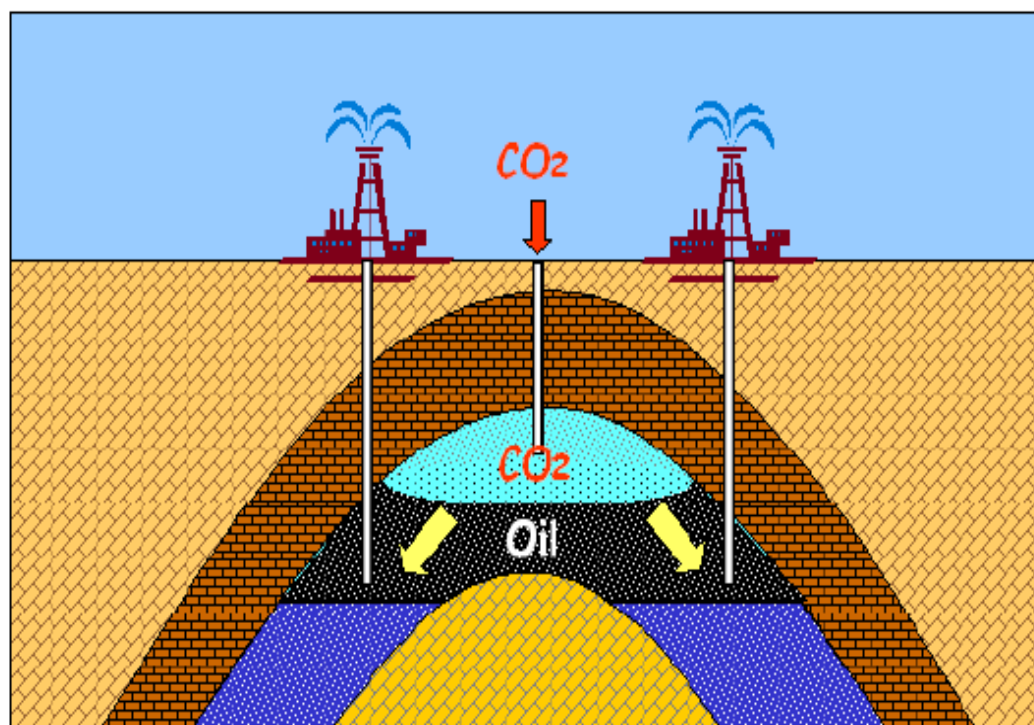


Figure 2.4. A Schematic of the Immiscible Displacement Technique (Peteves, 2018)

The presence of water in the reservoir diminishes the process' efficacy by impeding oil flow. As a result, this procedure may not be effective if used after a major flood. Because of the negative economics, the immiscible displacement process has only seen a few uses so far. While considerable volumes of CO<sub>2</sub> are required, as well as the construction of several new wells, increasing oil production remains gradual.

Before the project can start producing more oil, it may take up to ten years of injection. In addition, the reservoir is typically used for an immiscible project, which limits alternatives for relatively small implementation.

However, larger amounts of CO<sub>2</sub> can be stored in immiscible displacement projects than in miscible displacement projects. While the latter's ability to store CO<sub>2</sub> underground is constrained by the oil in which it dissolves and, to a lesser extent, by the oil and water that is left behind, the former's ability to store CO<sub>2</sub> underground is only constrained by the reservoir rock's porosity. While in miscible displacement operations, CO<sub>2</sub> breakout is unavoidable. Projects involving immiscible displacement may be created to prevent this, as it would be necessary to store CO<sub>2</sub> indefinitely.

### **Comparison of Immiscible and Miscible Displacement Processes.**

The main distinction between the two is in the case of immiscible CO<sub>2</sub> injection, vaporization of condensate by the injected CO<sub>2</sub> is the more effective mechanism for oil recovery. In the event of miscible CO<sub>2</sub> injection, miscibility is the main mechanism for the oil extraction. Assuming that WAG will exploit miscible projects and as long as the favourable pattern with water flooding persists, GSGI will take advantage of immiscible projects. Before activities are suspended, a miscible project can start at any time. GSGI immiscible projects, however, have a fundamentally unique good pattern, they can start close to the end of oil production. The major characteristics of the two approaches are summarized in Table 2.1 below.

Table 2.1.

*Comparison between miscible and immiscible displacement CO<sub>2</sub>-EOR techniques (Josendal, 2014)*

	<b>Miscible</b>	<b>Immiscible</b>
Oil xxtraction	Early (~1-4 years)	Late (>5-8 years)
Project scale	Smaller	Larger
Duration of Project	Short (<20 years)	Long (min. 10 years)
CO <sub>2</sub> recovery	Inevitable	Evitable
Potential recovery of oil	Lesser (4-11.5% OOIP)	Greater (~18% OOIP)
Potential storage of CO <sub>2</sub>	Lesser (53432 kg/MCF)	Greater (up to 178108 kg/MCF)
Experience	Significant	Less

## CO<sub>2</sub> Solubility in Simulated Live and Dead Oil

Oil displacement using CO<sub>2</sub> injection can be done in two ways; immiscible and miscible method and the difference between these two is MMP. MMP, according to Holm and Josendal (2014) earlier work, is the pressure that gives more than 4/5 of the oil present in the reservoir at the headway of the gas injected. Furthermore, MMP is associated with an oil recovery of at least 90% (Yellig & Metcalfe, 2018). In pressures below the MMP, the immiscible displacement mode occurs, whereby all the phases are mixed (Gozalpour, 2015). The gas and oil mingle in the reservoir, causing a part of the remaining oil in the formation to be mobilized (Zhang et al., 2018). As a result, the main principles behind immiscible flooding are viscosity and interfacial tension decrease, oil swelling, and a solution gas drive mechanism (Fath & Pouranfard, 2014; El-Hoshoudy & Desouky, 2018). A lot of transfer of mass can be used to provide miscible treatment at pressures above the MMP.

Some solvents like C<sub>2</sub>H<sub>6</sub>, make a separate phase at first when in contact with the fluid in the reservoir. While several contacts are possible when the oil vaporizes and the CO<sub>2</sub> condenses in the reservoir as a result of the vaporizing and condensing gas drive activities. (Verma, 2015; El-Hoshoudy & Desouky, 2018; Ostami et al., 2018). This creates a miscible phase between the oil and the CO<sub>2</sub> injected, and the residual oil becomes reduced. However, the immiscible CO<sub>2</sub> flooding cannot produce all of the reservoir fluid and a significant amount of the porous media can still have some residual oil saturation (Meyer, 2007). As a result, miscible method is commonly used in many countries for recovery of oil (Lake et al., 2019). Despite its common acceptability in oil projects, it does not work effectively for all reservoir. For example, the constituents of heavy oils that are vapourable will be inadequate to create expected miscible phase. Furthermore, in the event of light oil, the solubility pressure required may be higher than the formation fracturing pressure (Srivastava et al., 2017). To properly develop a CO<sub>2</sub>-EOR scenario, considerations must be taken for the oil composition and the reaction with the CO<sub>2</sub>. There have been numerous studies that have thrown light on the elements that influence the aforementioned parameter (Chung et al., 1988; Emera & Sarma, 2006; Welker, 2016; Rostami et al., 2017; Srivastava et al., 2017). In heavier oils the solubility of CO<sub>2</sub> is low (Emera & Sarma, 2006). Furthermore, when CO<sub>2</sub> dissolves it causes the oil to increase, with increasing pressure and as well as decreasing temperature (Miller & Jones, 1981; Briggs &

Puttagunta, 1984). However, it should be emphasized that in terms of oil solubility, gaseous CO<sub>2</sub> is superior to liquid CO<sub>2</sub> (Emera & Sarma, 2006; Kokal & Sayegh, 2019).

The practicality of a CO<sub>2</sub> injection scenario might benefit from a greater understanding of CO<sub>2</sub>-oil solubility. The most dependable methods for determining CO<sub>2</sub>-oil solubility are laboratory research. The experimental methods, on the other hand, take a lot of time and money (Emera & Sarma, 2006). Welker & Dunlop (2016) came up with an expression that linked solubility of CO<sub>2</sub>-oil with the API gravity using data from eleven dead oils. This device could only withstand pressures of up to 800 pounds per square inch, temperatures of up to 80 degrees Fahrenheit, and API gravities of 20 to 40 pounds per square inch. They also proposed the following association:

$$R_s = \frac{1000(SF - 1)}{0.345} \quad (2.1)$$

Where;

R<sub>s</sub>=solubility ratio

SF=swelling factor

Simon and Graue (2018) developed an improvement on the model in equation 2.1. Simon and Graue (2018), considered 9 dead oils and they established a correlation between the solubility of CO<sub>2</sub> in oil and its fugacity (</= 1800 psia), also known as Watson (2018) K factor (11–12.4), Temperature (100–250°F) and saturation pressure (≈ 2790 psia) are depicted in three graphical formats. Mulliken & Sandler (2018) used a combination of Peng-Robinson EOS (1976) and an oil characteristic that uses the oil's specific gravity and the UOP characterisation factor to determine R<sub>s</sub> and SF (or mean average boiling point). Mehrotra & Svreck (1985) proposed Equation 2.2:

$$R_s = -a - bP_s + c \left( \frac{P_s}{T + 273.15} \right) + d \left( \frac{P_s}{T + 273.15} \right)^2 \quad (2.2)$$

Where;

R<sub>s</sub> = solubility ratio

P<sub>s</sub> = saturation pressure

T = temperature

a, b, c, and d are constant parameters and correspond to the numbers 0.0073528, 14.792, 6425.7, and 4972.39, respectively. It's worth noting that the aforementioned association only applies to temperatures between 23.89 and 97.22 C and a pressure less than 6.38 MPa. Chung et al. (1988) expressed this as three added input factors that affect dissolving of CO<sub>2</sub> in dead oil:

$$R_s = 1 / [a\gamma^b T^c + dT^e \exp(-fP_s + g/P_s)] \quad (2.3)$$

Where;

R<sub>s</sub> = solubility ratio

P<sub>s</sub> = saturation pressure

T = temperature

0.4934E 2, 4.0928, 0.571E 6, 1.6428, 0.6763E 3, 781.334, and 0.2499 are the values for the parameters a through g, respectively. Experiments were conducted on heavy crudes from 5 hydrocarbon fields, including Bartlett (Kansas), and Chaffee (California), with API gravities ranging from 9 to 19. They considered pressure and temperature to be the most important factors influencing solubility. Despite providing plausible outcomes, the graphical and mathematical correlations given above have various shortcomings, including a sizable divergence from the experimental data. The limited dataset that represents the limited rock and fluid parameters as well as the experimental settings was used to produce the empirical correlations as well as all of their benefits. This phrase encapsulates the essence of contemporary techniques guiding the development of more universal and dependable models that may be used in a wide range of situations. Modelling the physical features of CO<sub>2</sub>-oil mixtures by using various machine learning genetic algorithm (GA) is a recurring issue in contemporary research fields.

Emera & Sarma (2006) extended on the findings by estimating properties of the oil and CO<sub>2</sub> mixtures, like; swelling factor, density, solubility, and viscosity using a variety of GA-derived correlations. CO<sub>2</sub>-oil solubility was calculated using temperature, saturation pressure, bubble point pressure, molecular weight (MW), and CO<sub>2</sub> liquefaction pressure. Based on oil and CO<sub>2</sub> states, the following connections were created:

- CO<sub>2</sub> in Dead Oil Solubility Equations Developed from GA

Gaseous state of CO<sub>2</sub> (P<sub>liq.</sub> < P<sub>i</sub>, T<sub>c,CO<sub>2</sub></sub> < T<sub>i</sub> and all P<sub>i</sub>; T<sub>c,CO<sub>2</sub></sub> > T<sub>i</sub>):

$$R_s \text{ (mole fraction)} = 2.238 + 0.33z + 3.236z^{0.64739} - 4.8z^{0.25656} P_s \quad (2.4)$$

$$\text{Where } z = \gamma \left( 0.006897 \frac{(1.8T+32)^{0.8}}{P_s} \right)^{\exp\left(\frac{1}{MW_o}\right)}$$

Liquid state of CO<sub>2</sub> (T<sub>c,CO<sub>2</sub></sub> > T<sub>i</sub> and P<sub>liq.</sub> < P<sub>i</sub>):

$$R_s \text{ (mole fraction)} = 0.033 + 1.14z - 0.7716z^2 + 0.217z^3 - 0.02183z^4 \quad (2.5)$$

$$\text{Where } z = \gamma \left( \frac{P_s}{P_{liq}} \right)^{\exp\left(\frac{1.8T+32}{MW_o}\right)}$$

- Expressions for Solubility of CO<sub>2</sub> in Live Oil obtained from GA

Gaseous state of CO<sub>2</sub> (T<sub>c,CO<sub>2</sub></sub> < T<sub>i</sub>, P<sub>i</sub> < P<sub>liq.</sub> and all P<sub>i</sub>; T<sub>c,CO<sub>2</sub></sub> > T<sub>i</sub>):

$$R_s \text{ (mole fraction)} = 1.748 - 0.5632z + 3.273z^{0.704} - 4.3z^{0.4425} \quad (2.6)$$

$$\text{Where } z = \gamma \left( 0.006897 \frac{(1.8T+32)^{1.125}}{P_s - P_b} \right)^{\exp\left(\frac{1}{MW_o}\right)}$$

The study of Rostami et al. (2017), modified the gene expression programme (GEP) method to approximating the mole fraction properly in terms of T<sub>i</sub> - temperature, P<sub>s</sub> - saturation pressure, P<sub>b</sub> - bubble point pressure, P<sub>liq.</sub> - liquefaction pressure, T<sub>c</sub> - critical temp., T<sub>R</sub> - reservoir temp., GEP - gene expression programming and MW -molecular weight (g/mole), to provide more insight CO<sub>2</sub> solubility in oil modelling. The model's use produced the following correlations between live and dead crudes:

- GEP-Based Model for the Solubility of CO<sub>2</sub> in Dead Oil

$$R_s \text{ (mole fraction)} = \frac{P_s T (a + b MW)}{c P_s^2 + d MW P_s T + T^2 + e \sqrt{T}} \quad (2.7)$$



Where 5.6444, 8.9318, 0.008756, 0.010819, and 41.105 are the corresponding values for the constant parameters a through e.

- GEP-Based Model for the Solubility of CO<sub>2</sub> in Live Oil

$$R_s \text{ (mole fraction)} = \frac{fP_b - gP_s + h}{iMW + jP_b - kP_s - \gamma T - A} \quad (2.8)$$

Where the values of the constants f through k are, respectively, 0.48618, 7.3713, 0.024262, 4.6233, 7.3695, and 5.03367. While A has this expression:

$$A = \begin{cases} 0 & \text{if } \gamma \leq 0.849 \\ 0.042756 & \text{if } \gamma > 0.849 \end{cases} \quad (2.9)$$

Rostami et al. (2018) used a monitored learning method, which is the least square support vector machine (LSSVM) technique, to carry out the above-mentioned experiment. They found reasonable agreement between their suggested models' projected CO<sub>2</sub>-oil solubility and experimental results for the two types of listed oils. Resilient Backpropagation (RB), Differential Evolution (DE), Scaled Conjugate Gradient (SCG), Genetic Algorithm (GA), and Firefly Algorithm were used to train the MLP and RBF predictors (FA). According to a widely disseminated dataset, the independent variables P<sub>s</sub>, P<sub>b</sub>, T<sub>i</sub>, MW, and z were used for the two listed oil types.

### **Records of CO<sub>2</sub> for EOR Projects**

In 2004, 79 CO<sub>2</sub>-EOR operations were operating around the world (Pierce, 2017). The majority of them are miscible CO<sub>2</sub>-EOR projects and one immiscible CO<sub>2</sub>-EOR project, were carried out in the US. Also, Canada has two ongoing CO<sub>2</sub>-EOR miscible displacement projects, Trinidad has five immiscible displacement simulated fields, and Turkey has one commercial immiscible displacement operation. In 2004, these projects generated a total of about 230000 barrels of oil per day, accounting for about 0.3 % of global oil production. A handful of modest CO<sub>2</sub>-EOR operations were operating in Hungary in the 1980s, but they were shut down in the mid-1990s (IEA Greenhouse Gas, 2020). The United States is clearly at the forefront of the method's application, accounts for more than 90 percent of the CO<sub>2</sub>-EOR oil output globally. Despite low oil prices, CO<sub>2</sub>-EOR output rose slowly in the 1970s and early 1980s but accelerated dramatically in the late 1980s and 1990s. There were three key causes for this (IEA Greenhouse Gas, 2020): (a) the decrease in recovery costs as a result of

technological advancements; (b) the lower cost of CO<sub>2</sub> due to its simple accessibility and supply from natural deposits (Schulte, 2014); and (c) the reorganization of oil corporations, which improved their capacity for cost-effective operation.

### **Lessons from Miscible CO<sub>2</sub>-EOR Operations**

A wealth of information and understanding about the physical and chemical principles underlying oil recovery has been gained as a result of the increasing records of miscible displacement projects. However, the general public does not have access to comprehensive information about the operational circumstances and performance of particular projects. The Permian basin in the United States is where the majority of the miscible displacement projects are located. There have also been created projects in the Midwest, the Gulf of Mexico, and the Rocky Mountain region.

The majority of these projects rely on CO<sub>2</sub> extracted from high-pressure, high-purity subterranean reserves. The McElmo dome in Colorado, for example, holds around 282.9 million m<sup>3</sup> of CO<sub>2</sub> at a pressure of approximately 13.5 MPa (IEA Greenhouse Gas, 2020). CO<sub>2</sub> extracted from industrial effluents is used in a small number of applications. The facilities supplied 5.7 million tons of CO<sub>2</sub> per year to EOR projects, according to a recent analysis (Gozalpour, 2015). The Rangely and Shanon Ridge EOR fields get 1.2 million tons of gas per year from two different gas processing plants in the United States. CO<sub>2</sub>-EOR operations have had varying degrees of success in a variety of reservoir situations (DTI SHARP, 2019a).

- Reservoirs (1000 m – 3000 m) both shallow and deep
- Reservoirs that are both tight and porous
- In carbonate reservoir rock and sandstone.
- Oils with low and medium viscosity (0.3 - 6 cp)

According to data from ten miscible displacement operations in the Permian region, the average net CO<sub>2</sub> injection into an oilfield is 163.9 m<sup>3</sup>/bbl of extra oil, which is the difference between the total CO<sub>2</sub> injection and the recycled CO<sub>2</sub>. According to research, this value varies between 134.2 m<sup>3</sup>/bbl in projects in the Rocky Mountains and 198.8 m<sup>3</sup>/bbl in projects in the Midwest (EPRI, 2015; IEA Greenhouse Gas, 2020). Overall, studies from a wide number of US operations imply that typical incremental oil recovery is between 4 and 12 percent OOIP, with the net amount of CO<sub>2</sub> injected being between 10 and 45 percent of the volume occupied by

hydrocarbons in the reservoir (DTI SHARP, 2019a). The adoption of the tapering WAG injection technique is associated with significantly higher oil recovery efficiencies (see Figure 2.2) (Schulte, 2014), where there is a progressive increase in the water to CO<sub>2</sub> ratio over time, with bigger starting CO<sub>2</sub> slugs and smaller end slugs. Not all oil reservoirs are suitable for CO<sub>2</sub>-EOR due to technological and financial considerations. Some generic principles for screening probable miscible displacement initiatives have been developed based on investigations conducted by other researchers:

- To ensure miscibility and reduce CO<sub>2</sub> usage, operation of the project must be above the MMP
- After water-flooding, at least 35–40% of the reservoir's capacity should be filled with the leftover oil (Schulte, 2014).
- The reservoir should have permeability of more than 100 mD, robust vertical connectivity, and moderate vertical heterogeneity (DTI SHARP, 2019b).
- Oil gravity should be greater than 35°API and viscosity should be between 1-2 cp.

Finally, despite the fact that numerous studies assert that an effective water flooding is a reliable sign of a positive CO<sub>2</sub>-EOR project, this is challenged because there is a substantial volume of water to be mobilized by CO<sub>2</sub> at the end of a water-flooding. Furthermore, CO<sub>2</sub> losses are high due to its breakdown into water (Ali, 2016). Furthermore, general issues with miscible displacement have been identified, which have failed in several projects:

- Inadequate research before beginning a project. Before a project can begin, the geology and petrophysics of the reservoir must be thoroughly studied. Due to (i) inadequate CO<sub>2</sub> sweep within the reservoir due to significant heterogeneities, (ii) low injectivity causes a delayed response, low recovery efficiency has resulted, (iii) due to a lack of understanding of the geology of the reservoir, gas can breakthrough early via high mobility routes (geological faults). This problem emphasizes the importance of thorough surveillance before the start of the project, as well as appropriate reservoir management.

- Lower reservoir pressure due to reduced injectivity, which could lead to a loss of miscibility and, as a result, a lower recovery efficiency. However, by raising injection rates in neighboring wells, the pressure can be restored.
- Wells and water pipes in an EOR project may stop working due to scale buildup. Higher calcium salt concentrations are produced in the oil water causing the pH lowered and the  $\text{Ca}^{2+}$  from limestones dissolved in the formation. Scale development and calcite precipitation are afterwards brought on by a decrease in surface pressure.
- The oxidation of  $\text{Fe}^{2+}$  components by  $\text{CO}_2$  in the presence of water yields carbonic acid which hasten corrosion (DTI SHARP, 2019a).

### **Lessons Learned from Immiscible $\text{CO}_2$ -EOR Operations**

Immiscible displacement projects have been established in a far less number than miscible displacement initiatives. Furthermore, the Bati oilfield in Turkey is the only significant project currently utilizing the method. The oilfield contains heavy oil with a low gravity (IEA Greenhouse Gas, 2020). Traditional oil recovery procedures only yielded approximately 1.45 percent of the OOIP, but since 1986, a natural reservoir has produced 6000 barrels of oil per day by  $\text{CO}_2$  injection. Expected ultimate recovery (EUR) is expected to recover approximately 6.5 percent of OOIP in total. The key mechanism for  $\text{CO}_2$ -EOR is its quick dissolving in oil ( $\approx 14 \text{ m}^3/\text{bbl}$ ), which makes possible the swelling of the oil even when no miscibility and low viscosity by a factor of ten. Approximately 1700 tons of  $\text{CO}_2$  have been injected every day since the experiment began, with 16 percent to 60% of it being recycled. The high  $\text{CO}_2$  solubility in unrecovered oil is the primary cause for  $\text{CO}_2$  retention underground. Furthermore, according to Pierce (2017), just an immiscible project of small size in the United States and five simulated prototype projects in Trinidad are now underway. In the past, several immiscible displacement pilot projects were started in the United States (e.g., the Bay St Elaine, the Weeks Island, and the Timbalier Bay projects) (Schulte, 2014), even though the simulated project yielded almost 59% of the oil remaining after water flooding (Advanced Resources International, 2015). In the 1980s and 1990s, several immiscible displacement operations were also managed in Hungary, benefiting from a local natural  $\text{CO}_2$  resource. In this case, EOR was carried out by constructing a synthetic gas cap that forced oil into the producing wells. Per barrel of extracted oil,  $380 \text{ m}^3$  (or  $760 \text{ kg}/\text{bbl}$ ) of  $\text{CO}_2$  were used overall.

The following conditions, according to experience, favour immiscible displacement (SHARP, 2017).

- The reservoir rock has a high vertical permeability.
- A significant quantity of oil to create a thick oil column.
- Within the reservoir, a sufficient lateral and vertical connectivity as well as a sharply dropping relief.

Despite lack of experience in immiscible displacement, the usage of CO<sub>2</sub> has been predicted to be in the range of 560–790 kg/bbl (DTI SHARP, 2019b; IEA Greenhouse Gas, 2020). Up to 20% of OOIP can be obtained using this method (DTI SHARP, 2019a).

### **Implementation Challenges for CO<sub>2</sub>-EOR**

Even though the technology to handle it is available, the application of CO<sub>2</sub> for oil recovery is not yet widely used in Europe. The main reasons for this include environmental concerns, ambiguous regulations, and poor cost performance. These concerns are highlighted in this section.

Many researchers have it taken upon themselves to carry out investigation on CO<sub>2</sub> capture separation which does have any to do with its application for oil recovery (Peteves, 2018). However, other have gone ahead further to considering its oil recovery application and the barriers of impurity that comes with as this impurities in it has a substantial influence on MMP. Also, this criterion for CO<sub>2</sub>-EOR operations will have a substantial impact on the development of high-capture-efficiency CO<sub>2</sub> capture devices.

### **CO<sub>2</sub> -Reservoir Interactions**

Despite the information acquired, it is still uncertain how the injected CO<sub>2</sub> will interact physically and chemically with the reservoir rock and its contents. Both the project's management and the quality of the oil extracted are impacted by this.

### **Influence on Project Effectiveness**

The effectiveness of a CO<sub>2</sub>-EOR operation could be decreased by scale development in the producer wells brought on by impurities in the mixture. Since the water from the producing wells contains more bicarbonate ions, CO<sub>2</sub> injection may

make calcium carbonate scaling worse by encouraging the build-up of calcite on tubing's walls and pores when the pressure decreases. Additionally, expansion could occur as the pressure of CO<sub>2</sub> increases in the production wells. As a result of the cooling, more asphaltenes may be deposited in the production wells, lowering injectivity. Depending on the degree of hotness of the well in relation with the reservoir and pressures, the impacts are reservoir-specific (Mahdaviara et al., 2021).

However, there is a lot of worldwide experience with using inhibitors to successfully deal with scaling issues if they occur. Scaling from calcium carbonate should also be minimal in the North Sea due to the modest number of carbonate reserves. Sandstones become more permeable in some formations, however, where the injected CO<sub>2</sub> dissolves minerals. Theoretically, channels forming will reduce the sweep efficiency when dissolution is severe, with unknown effects on the project's overall efficiency. This is significant for sandstones in particular because these minerals help cement the rock (Jiang et al., 2019).

### **Impact on Oil Quality**

A miscible displacement process, according to reports, tends to create lighter oil than the reservoir's initial crude. It's also been claimed that injecting CO<sub>2</sub> into the oil could raise the sulfur concentration. This is dependent on the amount of sulfur in the injected CO<sub>2</sub>. CO<sub>2</sub> collected from natural gas processing plants is used for EOR at the SACROC facility in West Texas. This is sour CO<sub>2</sub>, with a sulphur content of roughly 2%. However, new CO<sub>2</sub> capture plants can be designed to have minimal sulfur levels in the CO<sub>2</sub>. Sulfur content in coal ranges from 0.6 to 2.5 percent. A two-stage physical solvent procedure can be employed in a coal IGCC plant to clear the gas of any H<sub>2</sub>S. At first step 99.5 percent of sulfur is removed, Clean CO<sub>2</sub> can be captured in the second stage. If CO<sub>2</sub>-EOR is carried out using this clean CO<sub>2</sub>, the sulfur content of the generated oil is not affected by contaminants in the CO<sub>2</sub> which is being injected (Jiang et al., 2019).

### **Infrastructure Processes for CO<sub>2</sub> Capture, Cost Implication and Application**

The most significant impediment to CO<sub>2</sub>-EOR deployment in Europe has been the lack of low-cost CO<sub>2</sub> in adequate quantities. As previously stated, CO<sub>2</sub> must be gathered from nearby industrial source that emit it (Emera & Sarma, 2006). The economics of CO<sub>2</sub> capture has previously been examined in depth (Tzimas & Petevs,

2015). International experience with carrying CO<sub>2</sub> over long distances via pipeline is extensive. The integrated CO<sub>2</sub> pipeline system in West Texas transported over 25 million tons of CO<sub>2</sub> in 2003. The passage of CO<sub>2</sub> offshore will require protection of the pipelines from external corrosion caused by the marine system. However, pipeline coating technologies that resist marine corrosion have already had a lot of success in the North Sea (Tzimas & Georgakaki, 2005).

Even though CO<sub>2</sub>-EOR projects can generate large incremental oil sales, it takes around 5 years to have a breakeven for its operation. According to Schulte (2014), CO<sub>2</sub> buying accounts for 50% of the increased oil production expenses, while operating costs account for 37% and capital expenditures account for only 13%. Electricity, the primary factor in operational expenses is the energy used to power the production pumps and perform CO<sub>2</sub> separation, compression repeating, and re-injection in the wells (EPRI, 2015). Corrosion of iron infrastructure is a key issue when dealing with CO<sub>2</sub>. Once the CO<sub>2</sub> enters the injection well, it will need to be handled since CO<sub>2</sub> dissolves in water and produces carbonic acid. Carbon steels are corroded by carbonic acid. As a result, corrosion is a possibility for the annular producer wells' casing and tubing as well as the bottoms of the injector wells. It has been suggested that building new platforms rather than modifying current ones to make them CO<sub>2</sub> compliant would be a more cost-effective solution (Espie, 2017). Because some oilfields in the North Sea naturally contain considerable amounts of CO<sub>2</sub>, several wells have already been built to manage the effects of CO<sub>2</sub> corrosion. CO<sub>2</sub> corrosion is controlled in West Texas by using a polyethylene tubing lining.

The annulus is occupied with inhibitor which is the space between the tubing and casing, which has typically reduced corrosion to < 2.5µm/yr. An epoxy or fiberglass coating is frequently applied to the surface structures. The generated oil/CO<sub>2</sub>/water mixture is also collected using stainless steel manifolds. The specification of fields differ from one and another depending on the economic value of the well and the surrounding structure for its operation. As a result, it is currently very difficult to estimate the capital costs related to a particular field deployment. In some cases, it may be determined that the most cost-effective way to implement CO<sub>2</sub>-EOR would be to employ new platforms in the North Sea. FPSO (floating production storage and offtake) vessels have been used in more recently produced North Sea fields. It may be able to give EOR deployment in the North Sea considerable

flexibility or any other oil fields by using such vessels that are specifically equipped for CO<sub>2</sub>-EOR operations(Tzimas & Georgakaki, 2005).

Therefore, to overcome these barriers as listed above from the literature reviews, a suitable mechanism to recover as much oil as possible, it is necessary to evaluate the efficiency of CO<sub>2</sub>-enhanced oil recovery (EOR) and the formation for CO<sub>2</sub> sequestration capability using numerical simulation. The next chapter of this paper presents a numerical simulation using eclipse to model the possibility of CO<sub>2</sub>-enhanced oil recovery (EOR). The emphasis of the simulation findings will therefore be on highlighting how the features of the formation affect oil recovery and how much CO<sub>2</sub> is injected into the formation's hydrocarbon pores. The basic model for simulation will be built using petrophysical and hydrodynamic characteristics that are comparable to the field formation under consideration.



## CHAPTER III

### Methodology

#### Reservoir Description

In 1974, the Alwyn Field was found in the UK's East Shetland Basin of the North Sea, around 400 kilometres north of Aberdeen and 140 kilometres east of the closest Shetland Island. The distances between Strathspey, Alwyn, Ninian, and Dunbar fields are respectively 4 and 10 kilometres, 7 kilometres, and 10 kilometres south of each other. The lake is about 130 metres deep. The field is situated in UKCS Block 3/9 and extends into Block 3/4 to the north. Alwyn's position is depicted on the map in Figure 3.1.

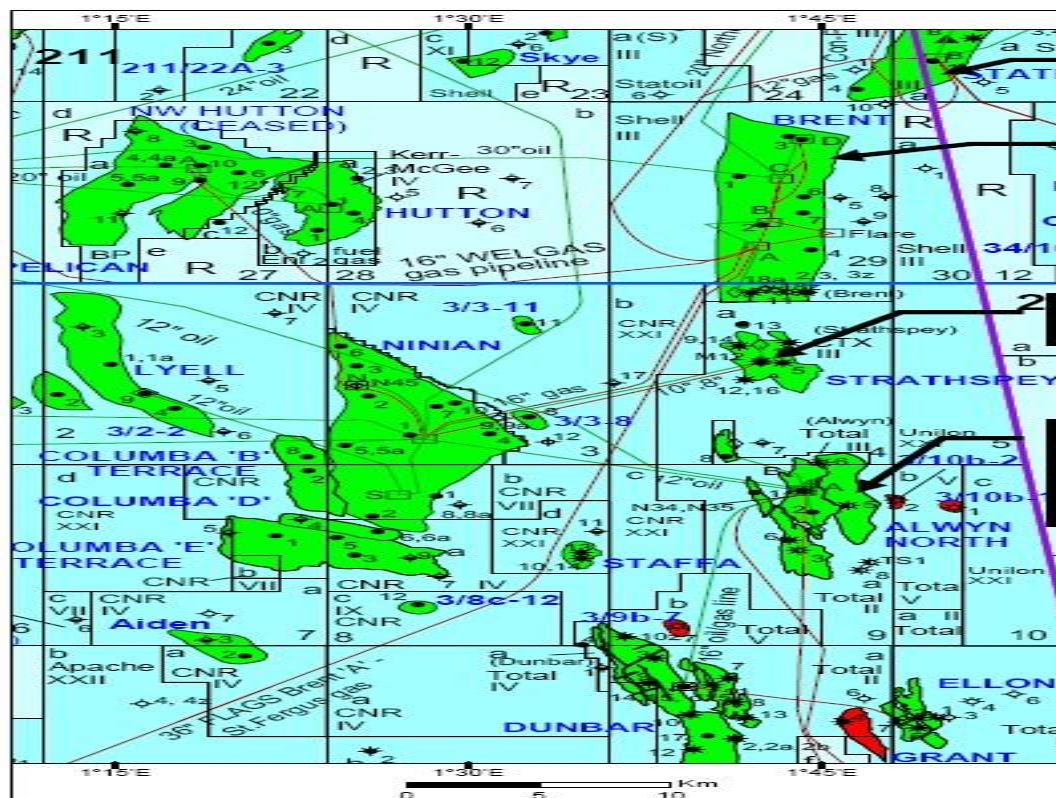


Figure 3.1. *Alwyn Field Localization Map (Amadi et al., 2020)*

This research will solely focus on the Alwyn Field's East Panel. In order to fully understand the geology of the Alwyn Field, a detailed field geological description was required. The Brent East Block of the Alwyn field has four

boundaries: the east, south, and west bounds are defined by the Base Cretaceous Unconformity (BCU), the central west limit is defined by the Spinal Fault, and the northern boundary is defined by a fault with a minor throw. The three primary units of the Brent group are Lower Brent (Broom, Rannoch, and Etive formations), Upper Brent (Broom, Rannoch, and Etive formations) and Middle Brent (Ness formations), which are all Tarbert formations. The last two formations are the only ones that produce oil in the Brent East panel.

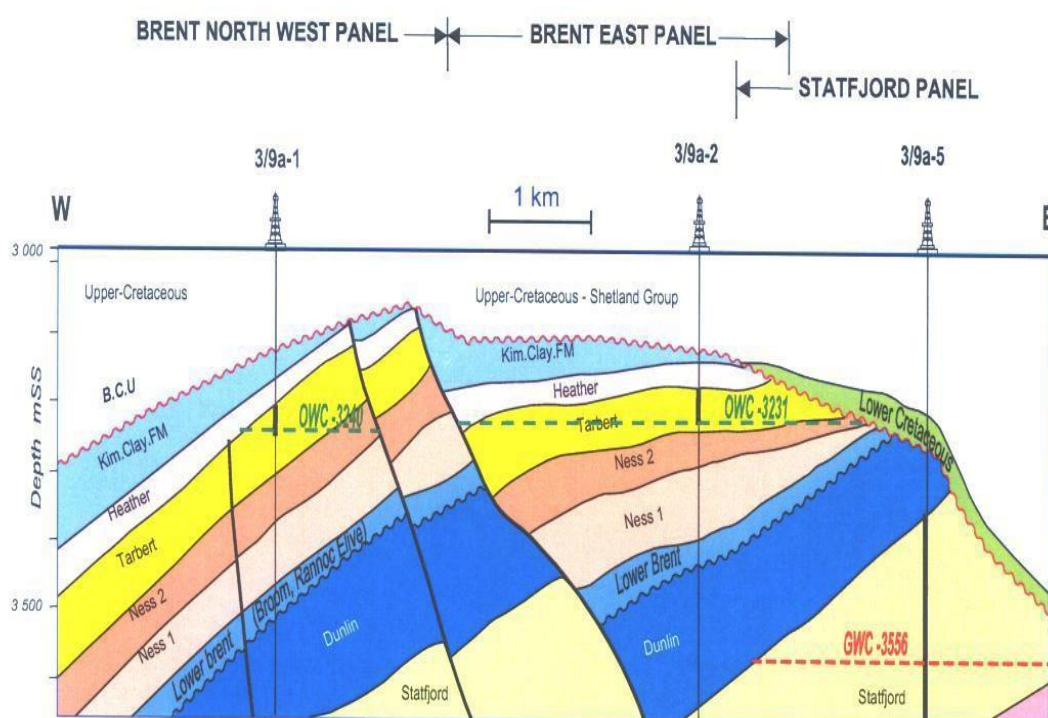


Figure 3.2. *Brent Geological Cross Section (Amadi et al., 2020)*

The Brent East reservoir in the Alwyn field was described using information from two of the initial vertical appraisal wells (3/9A-4 and 3/9A-2) and two new deviated delineation wells (Z1 and Z3). Z3 was typical of the northern half of the field, where a sizable oil leg was mostly present in the Tarbert units. Z1 in the west only encountered an active aquifer and failed to generate any oil.

### **Reservoir Model Characteristics**

A reservoir simulation model was created based on the Brent East features reported before to study the reservoir's production performance. The initial reservoir model was created using the Y2, Y4, Z2, and Z3 appraisal wells. Depending on the

production/injection requirements, these wells may be utilised or abandoned. A black oil model in eclipse was built using rectangular cells with 51 cells on the y direction, 36 cells on the x direction and 18 cells along z-direction, due to a hazy understanding of the Brent East reservoir at the start of the project. The reservoir's shape is specified in the Petrel file "MODEL PETREL.GRDECL." The spinal fault geometry and the north fault limit serve as the structural foundation for the corner point geometry.

### **Reservoir Simulation**

The purpose of the simulation was to measure reservoir production performance of Alwyn during miscible CO<sub>2</sub> injection. The results would be compared to other recover scenario/cases. The three-comparison case includes;

- Natural depletion
- Immiscible gas injection
- Miscible CO<sub>2</sub> injection

The simulation software of choice is Eclipse. The Eclipse simulator suite is made up of two different simulators: Eclipse 100 for black oil modelling and Eclipse 300 for compositional modelling. Eclipse 100 is a three-phase, three-dimensional, general-purpose black oil simulator with gas condensate options that is completely implemented (Schlumberger, 2010).

### **Miscible Injection Modeling**

When there is no phase barrier or interface between the reservoir oil and injected fluid, miscible displacement is said to occur. To model the miscible CO<sub>2</sub> injection, the Eclipse solvent Todd and Longstaff model extension would be utilized instead of a compositional model, which would be more complex (Schlumberger, 2010). The solvent extension of this study adopts the Todd- Longstaff empirical model used during miscible flooding.

### **The Todd and Longstaff Mixing Parameter Model**

Todd Longstaff's model is an empirical analysis of the effects of miscible component dispersion in the hydrocarbon phase. The model includes a parameter ( $\omega$ ), whose value varies from 0 to 1, to represent the size of the dispersed zone in each grid

cell. The amount of fluid mixed in each grid cell depends on the value of this variable. A value of 1 is used when the size of the zone scattered is significantly larger than the size of a typical grid cell and the hydrocarbon component can be considered completely mixed in each grid (Todd & Longstaff, 1972). The miscible components in this situation have the same density and viscosity. The mixing rule equations lead to the Todd and Longstaff mixing parameter model. The miscible components should have the same viscosity and density as the pure components because a value of  $\omega = 0$  is used to represent the effect of a very thin dispersed zone between the gas and oil components. In real applications, an intermediate value of would be required to approximate the miscible components when they are incompletely mixed (Todd & Longstaff, 1972). In the omega parameter, the Todd-Longstaff model interpolates between two images of phase viscosities. Each phase has its typical viscosity value when  $\omega = 0$ . Miscible phases have a common mixed viscosity, which is a power-law combination of the separate phase viscosities, where  $\omega = 1$ .

$$\mu_{oe} = \mu_o^{(1-\omega)} \mu_{om}^{\omega} \quad (3.1)$$

$$\mu_{ge} = \mu_g^{(1-\omega)} \mu_{gm}^{\omega} \quad (3.2)$$

$$\mu_{se} = \mu_s^{(1-\omega)} \mu_{sm}^{\omega} \quad (3.3)$$

Where the mixed viscosities are:

$$\mu_{om}^{\omega} = \frac{\mu_s \mu_o}{\left( \frac{S_o}{S_{os}} \mu_s^{1/4} + \frac{S_s}{S_{os}} \mu_o^{1/4} \right)^4} \quad (3.4)$$

$$\mu_{gm}^{\omega} = \frac{\mu_s \mu_o}{\left( \frac{S_g}{S_{gs}} \mu_s^{1/4} + \frac{S_s}{S_{gs}} \mu_g^{1/4} \right)^4} \quad (3.5)$$

$$\mu_{sm}^{\omega} = \frac{\mu_s \mu_o}{\left( \frac{S_g}{S_n} \mu_o^{1/4} \mu_s^{1/4} + \frac{S_o}{S_n} \mu_g^{1/4} \mu_s^{1/4} + \frac{S_s}{S_n} \mu_o^{1/4} \mu_g^{1/4} \right)^4} \quad (3.6)$$

Where;

$\mu_g$  = viscosity of gas

$\mu_o$  = viscosity of oil

$\mu_s$  = viscosity of solvent

$\mu_{gm}$  = fully mixed viscosity of gas + solvent

$\mu_{om}$  = fully mixed viscosity of oil + solvent

$\mu_{sm}$  = fully mixed viscosity of oil + gas + solvent

$\omega$  = Todd – Longstaff Parameter

$$S_n = S_{gas} + S_{oil} + S_{solvent} \quad (3.7)$$

According to Todd and Longstaff, the effective phase density, which appears in Darcy flow formulas, is likewise a combination of the real phase densities. The fact that the phases are seen as linked and flowing as one is reflected in this. In the completely miscible case with  $\omega = 1$  both the viscosities and densities of the phases must match, so that they flow as if they were components of a single phase.

$$\left(\frac{S_o}{S_n}\right)_{oe} = \frac{(\mu_{oe}^{1/4} \mu_s^{1/4}) - (\mu_s^{1/4} \mu_o^{1/4})}{\mu_{oe}^{1/4} (\mu_o^{1/4} - \mu_s^{1/4})} \quad (3.8)$$

$$\left(\frac{S_g}{S_n}\right)_{ge} = \frac{(-\mu_{ge}^{1/4} \mu_s^{1/4}) - (\mu_s^{1/4} \mu_g^{1/4})}{\mu_{ge}^{1/4} (\mu_s^{1/4} - \mu_g^{1/4})} \quad (3.9)$$

$$\left(\frac{S_s}{S_n}\right)_{ge} = \frac{(S_{of} \mu_o^{1/4} \mu_g^{1/4}) - \left(\frac{\mu_o^{1/4} \mu_g^{1/4}}{\mu_{se}^{1/4}}\right) + (S_{gf} \mu_o^{1/4} \mu_s^{1/4})}{(S_{of} \mu_o^{1/4} \mu_g^{1/4}) - (\mu_o^{1/4} - \mu_g^{1/4}) + (S_{gf} \mu_o^{1/4} \mu_s^{1/4})} \quad (3.10)$$

The effective gas, oil and solvent densities ( $\rho$ ) are calculated from the effective saturation fractions in equations 3.11 to 3.13.

$$\rho_{ge} = \rho_g \left( \frac{S_g}{S_n} \right)_{ge} + \rho_s \left( 1 - \left( \frac{S_g}{S_n} \right)_{ge} \right) \quad (3.11)$$

$$\rho_{oe} = \rho_o \left( \frac{S_o}{S_n} \right)_{oe} + \rho_s \left( 1 - \left( \frac{S_o}{S_n} \right)_{oe} \right) \quad (3.12)$$

$$\rho_{se} = \rho_s \left( \frac{S_o}{S_n} \right)_{se} + \rho_g S_{gf} \left( 1 - \left( \frac{S_o}{S_n} \right)_{se} \right) + \rho_o S_{of} \left( 1 - \left( \frac{S_o}{S_n} \right)_{se} \right) \quad (3.13)$$

Where;

$$S_{of} = \frac{S_{oil}}{S_{oil} + S_{gas}} \quad (3.14)$$

$$S_{gf} = \frac{S_{gas}}{S_{oil} + S_{gas}} \quad (3.15)$$

$\rho_{ge}$  = density of effective gas

$\rho_g$  = density of gas

$\rho_{oe}$  = density of effective oil

$\rho_{se}$  = density of effective solvent

$\rho_s$  = density of solvent

$\rho_o$  = density of oil

### Model Assumptions and Constraints

The model assumptions and constraints for natural depletion, immiscible gas injection and finally miscible CO<sub>2</sub> injection are as follow:

### ***Case 1: Natural Depletion***

- There is no water influx into the reservoir due to a lack of aquifer support.
- Rock and liquid expansion are used for recovery.

### ***Case 2: Immiscible Gas Injection***

- It is possible to inject lean Statfjord gas.
- The characteristics of this lean gas are thought to be similar to those of Brent dissolved gas.
- The maximum gas injection rate per well is 800,000 Sm<sup>3</sup>/d.
- A total gas injection capacity of 3,200,000 Sm<sup>3</sup>/d was available.
- Voidage replacement is used to control injection.

### ***Case 3: Miscible CO<sub>2</sub> Injection***

- Solvent (CO<sub>2</sub>) injection was followed by pressurization by injecting water in a 3 months interval.
- 3,000 Sm<sup>3</sup>/d was the maximum water injection rate per well.
- The total amount of water that can be injected was 15,000 Sm<sup>3</sup>/ d.
- The total maximum injection gas available was 3,200,000 Sm<sup>3</sup>/ d.
- The maximum injection gas rate per well was 800,000 Sm<sup>3</sup>/ d.

### **PVT Data**

In this study, a black oil PVT was used. The required composite black oil PVT data is contained in the PVT data file 'PVT.INC,' which accounts for the field separation conditions. The initial PVT values of the reservoir fluid are shown in the Table 3.1.

Table 3.1.

*Parameters used for reservoir simulation on the Alwyn Field (Amadi et al., 2020)*

<b>Properties</b>	<b>Unit</b>	<b>Value</b>
Initial reservoir pressure	Bar	446
Injection pressure	bar	475
Reservoir temperature	F	233
Average reservoir porosity	%	21
Average reservoir permeability	md	1000
Reservoir datum depth	m	3200
Oil-water contact	m	3231
Oil density	kg/m <sup>3</sup>	1.87
Gas-oil contact	rb/stb	500
Initial oil formation volume factor	bar	1.61
Bubble point pressure	rb/stb	258.2
Formation volume factor @ saturation pressure	rb/stb	1.69
Oil formation volume factor	v/v	1.64
Gas oil ratio	ft <sup>3</sup> /bbl	206.9
API gravity	API	39
Viscosity of saturated oil	cp	0.31
Water viscosity @ 112c	cp	0.35
Water viscosity @ 50c	cp	0.31
Oil viscosity	cp	0.4
Oil viscosity @ 340bars	cp	0.35



## CHAPTER IV

### Result and Discussion

#### Findings

The simulation case for natural depletion, gas injection, and miscible gas injection was simulated in Eclipse 100 in order to evaluate the reservoir performance of the Alwyn field for each production scenario. Figure 4.1 shows the grid and geometry of the Alwyn field extracted from Petrel.

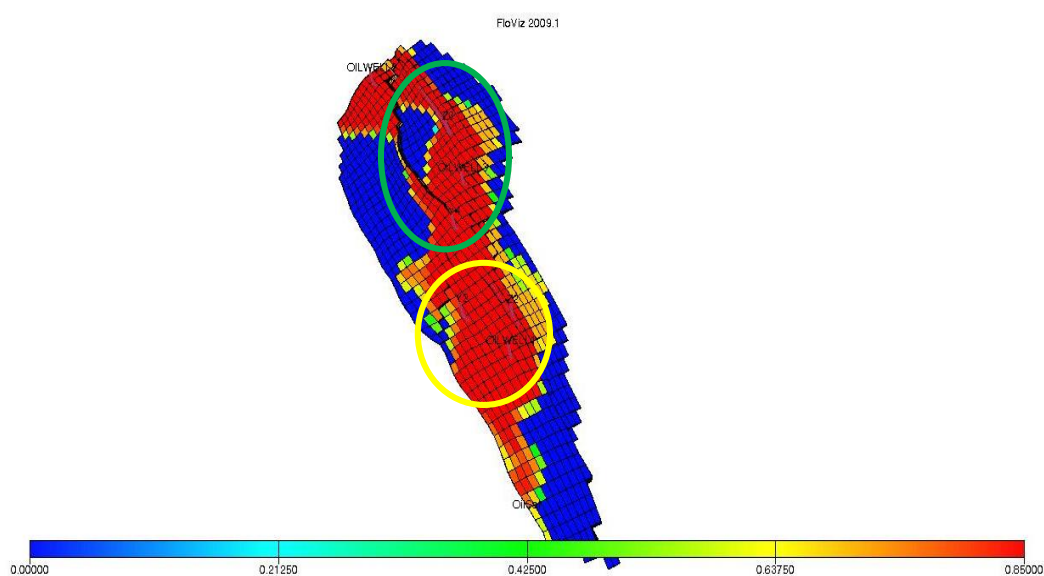


Figure 4.1. *Faults in the Alwyn Field (Non-transmissible Fault in Yellow, Transmissible Fault in green) (Generated by Floviz)*

Two faults running from north to south are captured in the model. The north dominated fault was found to be non-sealing while the southern fault was sealing. This made production from down south low compared to other regions. Four development wells (Y2, Y4, Z3, Z4) were used to do a pre-simulation of reservoir performance without any additional well. Figure 4.2 shows the position of the wells. Z2 and Z3 are deviated wells Z3 was drilled to target accumulations in the up north separated by the northern fault.

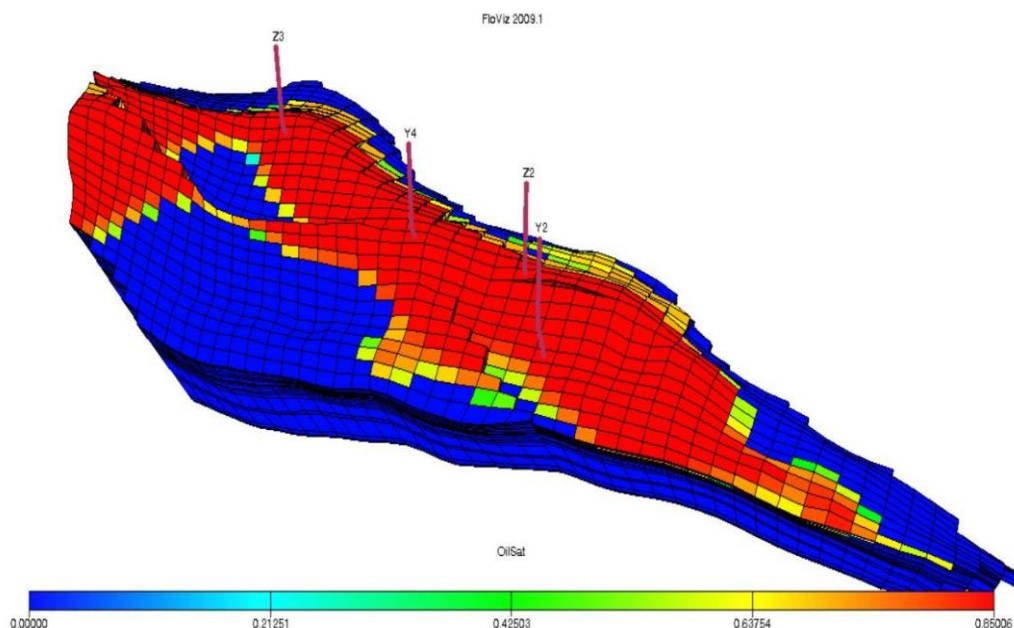


Figure 4.2. *Well Position for Initial Development Scenario (Generated by Floviz)*

Figure 4.2 displays the visual oil saturation of the reservoir after simulation for 10 years. The scale shows that the field is poorly produced as oil saturation is still about 0.8 (80%) on average. Giving a justification to drill more wells and use other development techniques to improve the recovery from the field.

### **Natural Depletion**

The act of producing hydrocarbons from an oil or gas reservoir without using any procedure (such as fluid injection to increase the inherent energy of the reservoir) is known as natural depletion. This natural energy may result from a water drive, gravity drainage, aquifer and rock expansion, or solution gas drive (Green and Willhite, 2018). However, this energy might not be sufficient enough to sustain optimum oil production, especially in the case of a reservoir whose initial energy is solution gas drive. In this section, we will discuss the oil production scheme via the natural energy of the reservoir using the Eclipse simulator for simulation.

In this scenario, we simulated in Eclipse the behaviour of the reservoir under natural depletion and the expected recovery. The model was run by using a flowing bottom hole pressure of 100 bar (BHP), as specified in the production constraint. Plateau rate was to be maintained at 3200 Sm<sup>3</sup>/d for 4 years with wells producing at 1800 Sm<sup>3</sup>/d or 2400 Sm<sup>3</sup>/d for vertical and directional drilled wells respectively.

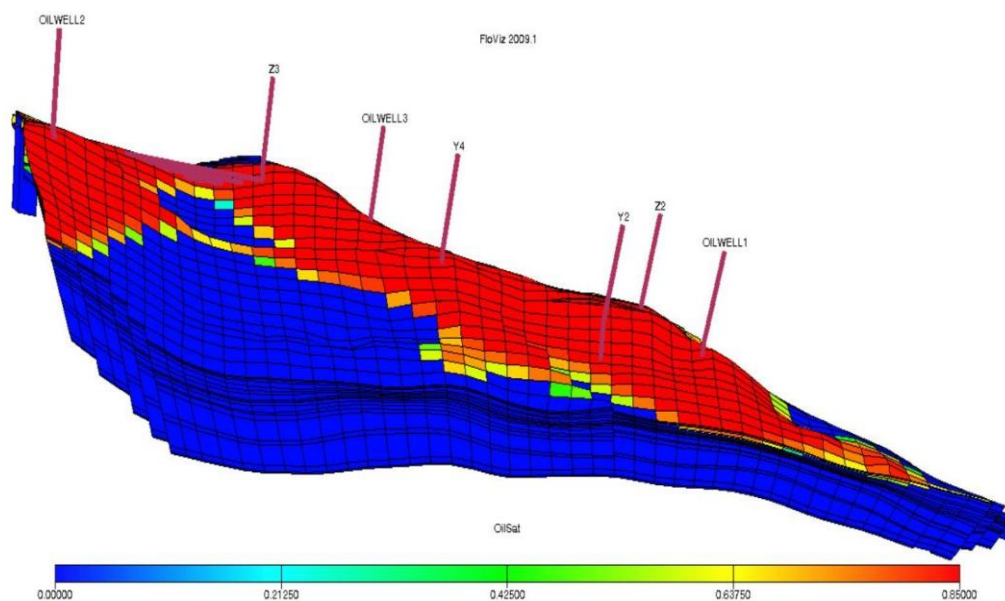


Figure 4.3. Well Position for Gas Natural Depletion Scenario (Generated by Floviz)

Table 4.1.

*Position and grid geometry of wells for natural depletion*

Well	I	J	Phase	Status	Geometry	Rate (Sm <sup>3</sup> /d)
Z2	11	26	Oil	Producer well	Deviated	2400
Z3	20	13	Oil	Producer well	Deviated	2400
Y4	12	21	Oil	Producer well	Vertical	1800
Y2	6	28	Oil	Producer well	Vertical	1800
OILWELL1	8	33	Oil	Producer well	Vertical	1800
OILWELL2	14	2	Oil	Producer well	Vertical	1800
OILWELL3	17	18	Oil	Producer well	Vertical	1800

The simulated model consists of four appraisal wells Y4, Y2, Z2, and Z3, and three new vertical production wells OILWELL1, OILWELL2, and OILWELL3 positioned strategically for optimum recovery. Well Y2 had low oil productivity due to high water production because it was completed (perforated) below the water table. Productivity from Y2 was also impaired due to poor transmissivity resulting from the southern sealing fault. Well efficiency was kept at 90% using the keyword WEFAC to account for 10% downtime due to maintenance of each well. Figures 4.4 to 4.6

show the depletion of field after producing with natural depletion injection and poor oil production of well Y2.

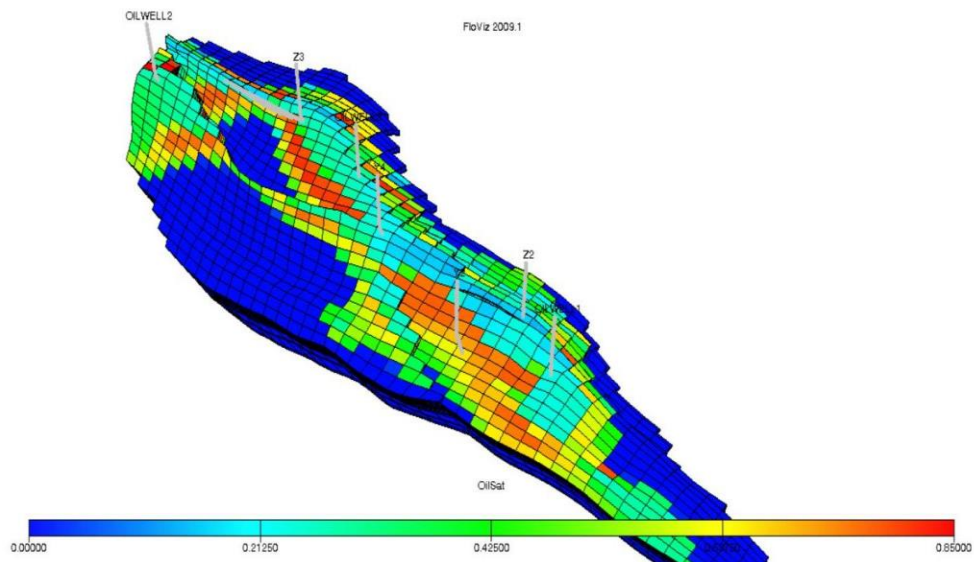


Figure 4.4. Depletion of Field after Producing with Natural Depletion Injection (Generated by Floviz)

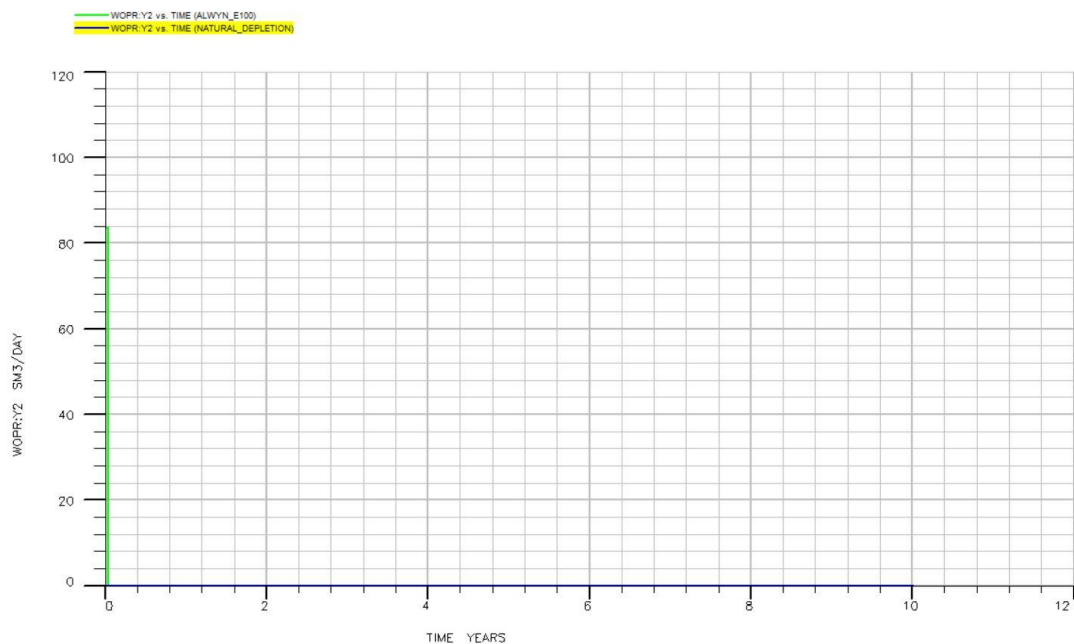


Figure 4.5. Poor Oil Production from Well Y2 (Later Converted to a Gas Injector) (Generated by Floviz)

Regardless of the wells' structural positions, all of them exhibit a fast rising gas-oil ratio during this natural depletion. Following a drop in reservoir pressure

below the bubble-point pressure, gas begins to form from solution throughout throughout the reservoir. Free gas starts to flow toward the wellbore after the gas saturation surpasses the critical gas saturation, and the gas-oil ratio rises (Amadi et al, 2020).

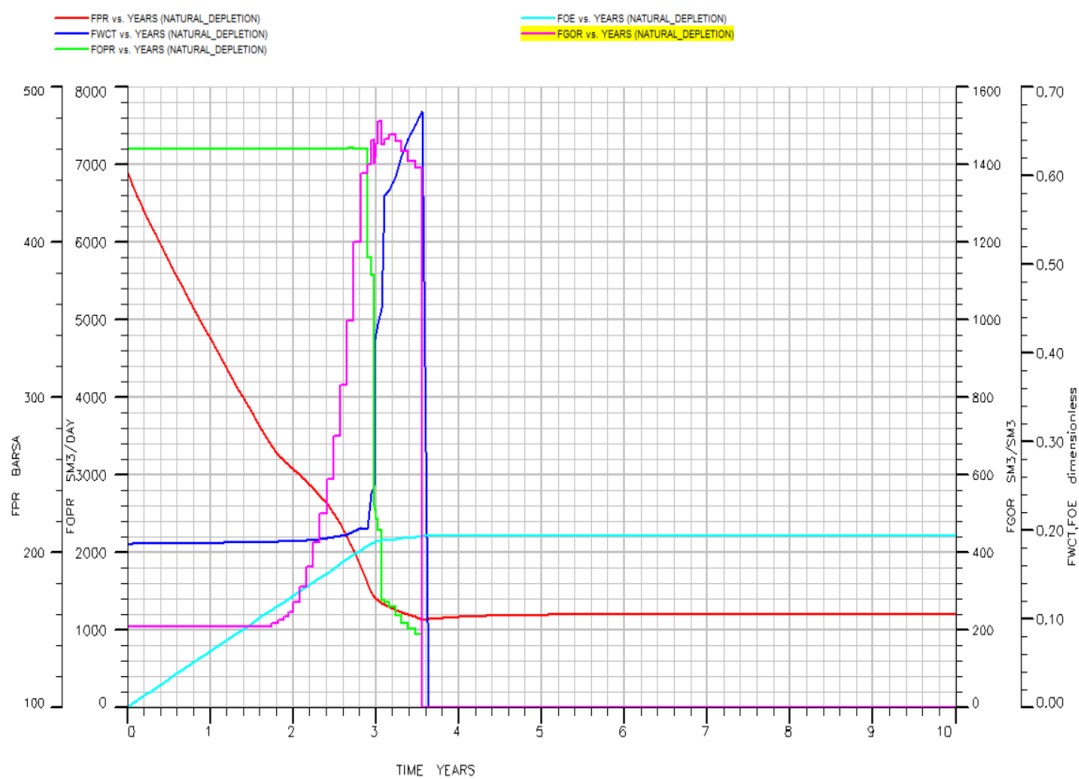


Figure 4.6. Plot of FOPR, FGOR, FWCT, and FPR for Natural Depletion (Generated by Floviz)

The maximum field production per day is shown in Figure 4.6 to be fixed at 7200 Sm<sup>3</sup>/d. This rate was maintained for almost 3 years before it rapidly decreased due to a decline in reservoir pressure. The reservoir's pressure was reduced to roughly 160 bars, and the final recovery was 19%. Poor output from the positioned well Y2 (as indicated in Figure 4.5) can also be blamed for the reduced recovery factor (FOE). There was still more oil in the reservoir, but due to the low reservoir pressure, production was not possible, thus this recovery is quite low (Green & Willhite, 2018). Rapid and sustained pressure loss occurred in the reservoir. This behaviour of the reservoir pressure is related to the lack of gas caps or extraneous fluids that may replace the gas and oil withdrawals. Therefore, it is crucial to keep the reservoir pressure as high as possible throughout production, preferably above the reservoir

fluid's bubble point. Technically, this process is known as pressure maintenance (Green & Willhite, 2018).

The field gas-oil ratio (FGOR) and field water cut (FWCT) plot is also displayed in Figure 4.6. As seen from this curve the maximum FGOR is  $1500 \text{ Sm}^3/\text{Sm}^3$  it increased rapidly with the reduction in pressure below the bubble point (258.2 bars), as FWCT increased to 67%.

### Immiscible Gas Injection Development Scheme

The gas was considered to possess the same properties as the dissolved gas in Brent. Voidage replacement was the control. The critical saturation of the gas was set to zero as the gas is expected to be immediately mobile upon injection. Well Y2 was converted to a gas injector as the previous simulation from the Natural depletion scenario showed it was a poor producer.

The gas scenarios were achieved by drilling two gas injectors (GASINJ1 and GASINJ) locating the best well position to improve oil recovery and optimize production. The gas injection scheme was constrained to an economic BHP of 100 bars. The field was constrained to a field gas injection rate of  $3,200,000 \text{ Sm}^3/\text{d}$  with each injector well limited to a surface rate of  $800,000 \text{ Sm}^3/\text{d}$  at an injection pressure of 475 bars. Figure 4.7 shows the positions of the wells.

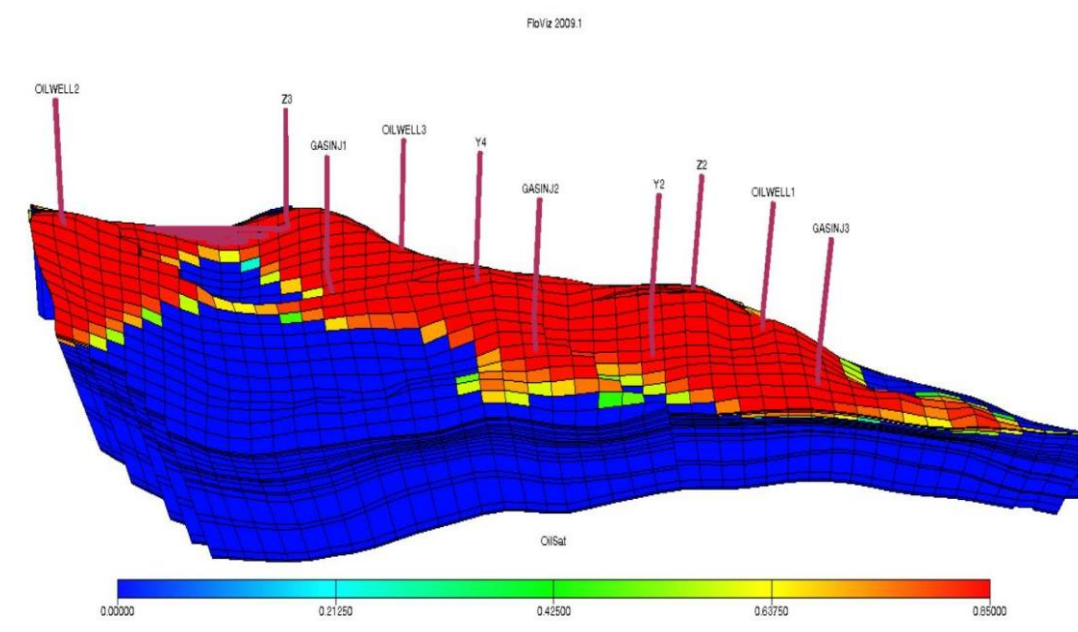


Figure 4.7. Well Position for Gas Injection Scenario (Generated by Flviz)

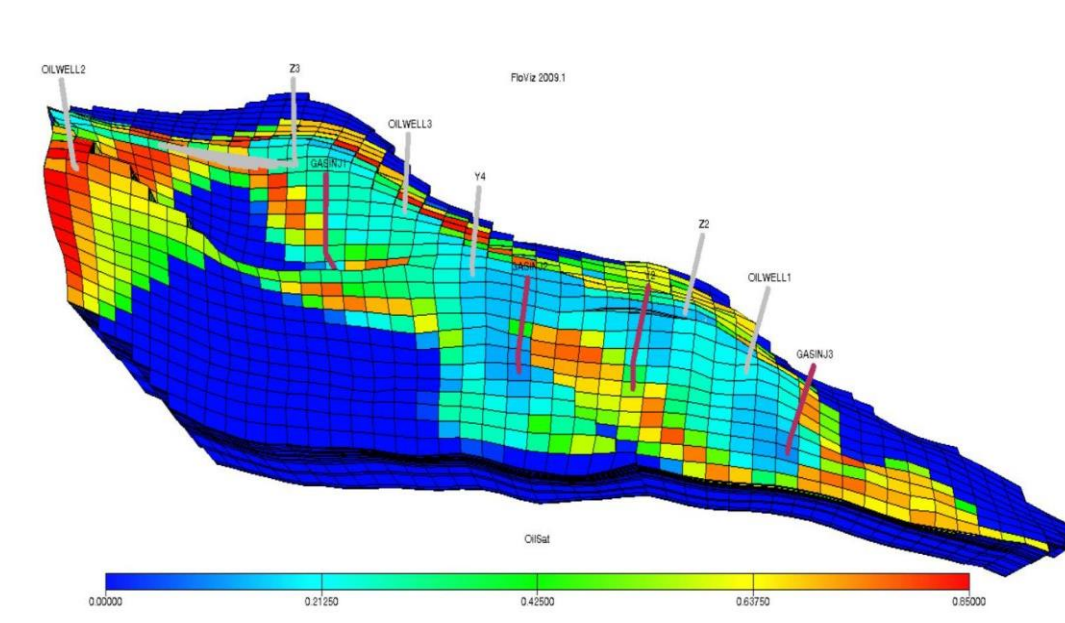


Figure 4.8. Depletion of Field after Producing with Gas Injection (Generated by Flviz)

Figure 4.8 depletion plot after simulation for a 10-year period. The simulated model consists of four appraisal wells Y4, Y2, Z2, and Z3, and three new vertical production wells OILWELL1, OILWELL2, and OILWELL3 positioned strategically for optimum recovery. Three vertical gas injection GASINJ1, GASINJ2, and GASINJ3 were also drilled, making a total of 6 production wells and 4 injection wells. Table 4.2 shows the positions of the wells.

Table 4.2.

*Position and grid geometry of wells for gas injection*

Well	I	J	Phase	Status	Geometry	Rate (Sm <sup>3</sup> /d)
Z2	11	26	Oil	Producer well	Deviated	2400
Z3	20	13	Oil	Producer well	Deviated	2400
Y4	12	21	Oil	Producer well	Vertical	1800
Y2	6	28	Gas	Injector well	Vertical	1800
OILWELL1	8	33	Oil	Producer well	Vertical	1800
OILWELL2	14	2	Oil	Producer well	Vertical	1800
OILWELL3	17	18	Oil	Producer well	Vertical	1800
GASINJ1	13	15	Gas	Injector well	Vertical	800000
GASINJ2	6	23	Gas	Injector well	Vertical	800000
GASINJ3	3	35	Gas	Injector well	Vertical	800000

Well Y2 was converted to a gas injector well, due to excess water production and low productivity as indicated in the natural development case scenario. The lower zones of well Y2 was which was perforated in the water bearing sands was plugged off and it was converted to a gas injector. Field gas injection plot showed a stable maximum gas injection rate for 5 years, indicating good injectivity from the wells as shown in Figure 4.9.

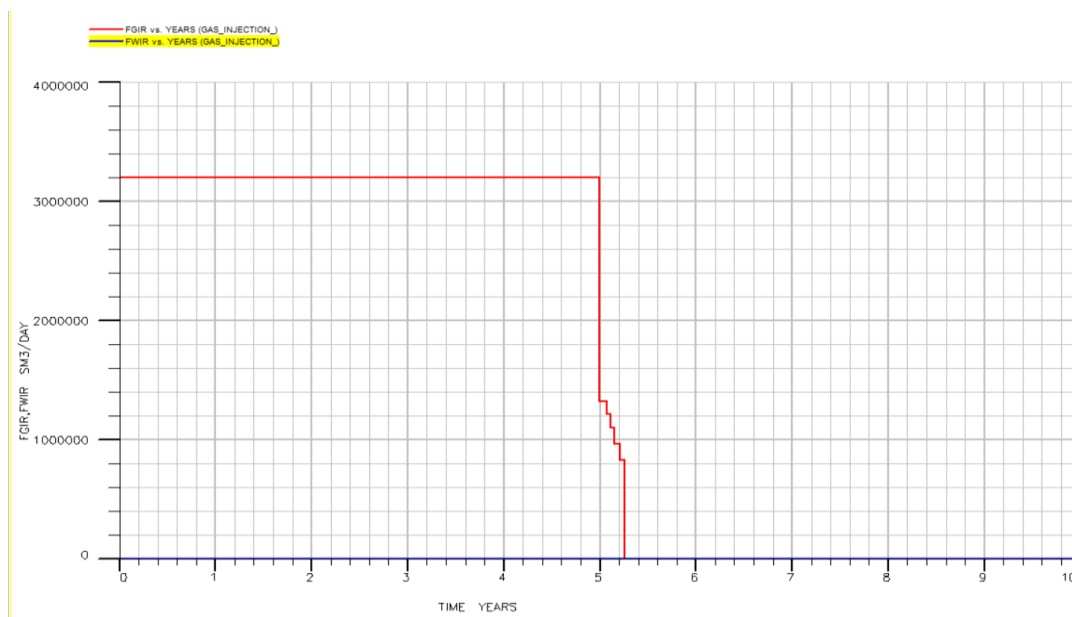


Figure 4.9. *Field Gas Injection Profile for Gas Injection Scenario (Generated by Floviz)*

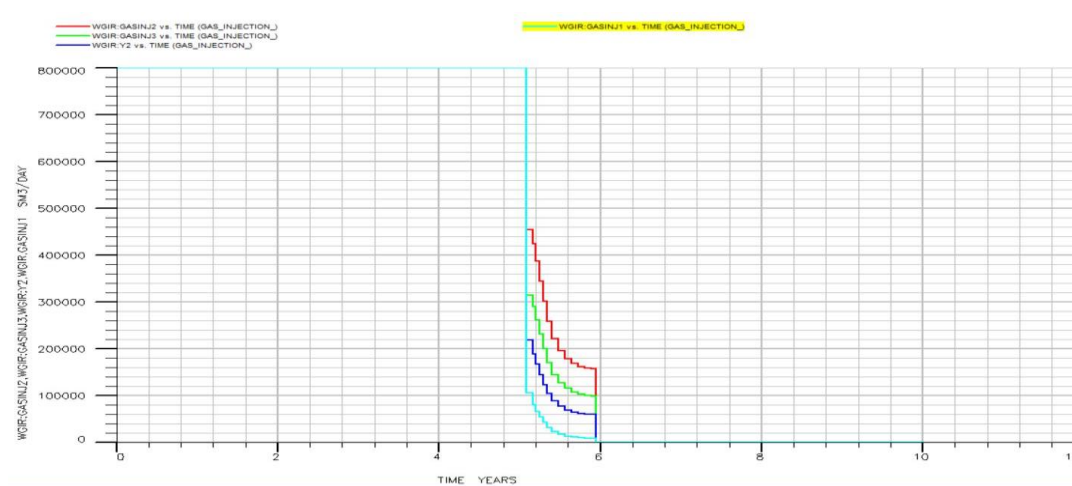


Figure 4.10. *Gas Injection Wells Plot (Y2 shows more potential contribution as an Injector) (Generated by Floviz)*



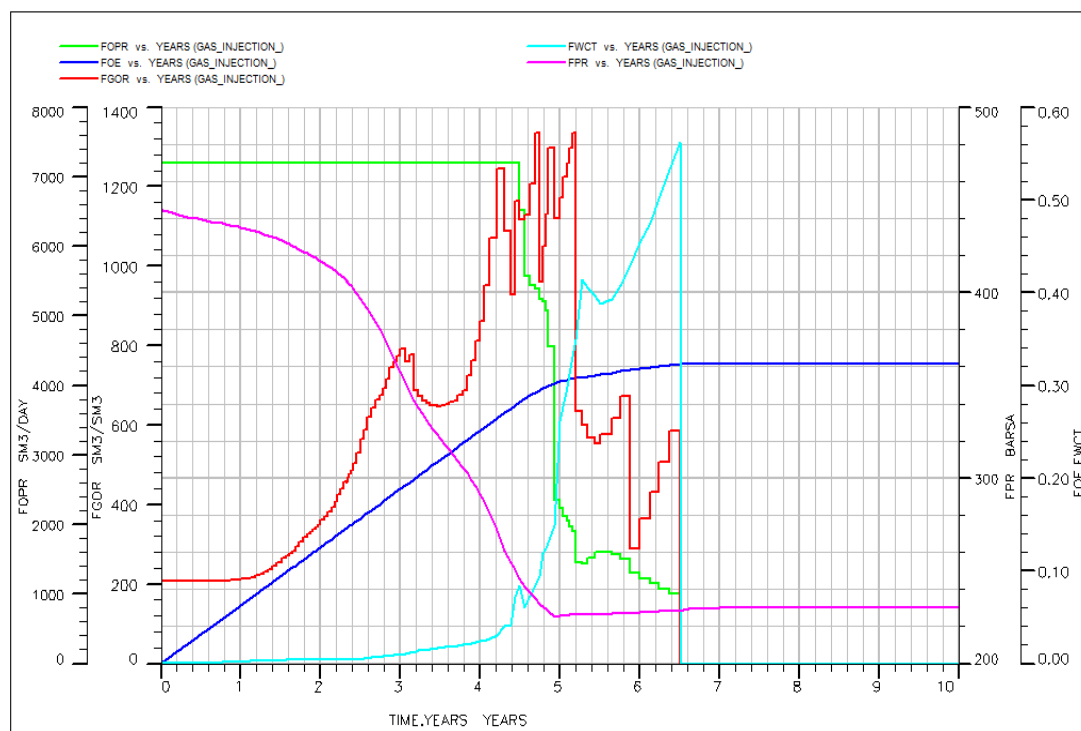


Figure 4.11. *Field Performance Plots for Gas Injection Scenario (Generated by Floviz).*

Figure 4.11 shows the reservoir performance in terms of oil flow rate, pressure, gas oil ratio water cut, and oil recovery. From Figure 4.11, it can be seen that there was less water production as field water cut was about 56% after 6 years of production. Consistent with the observations by Amadi et al. (2020), there was an early gas breakthrough at pressures above saturation pressure, and the gas-oil ratio increased. Oil recovery by gas injection yields a considerably larger recovery efficiency than that of natural depletion. The plateau was maintained for up to 4.5 years before declining rapidly. The field was produced for about 6.5 years before shutting down. Oil recovery was 32%.

### Miscible Gas (CO<sub>2</sub>) Injection

Miscible gas injection involves injecting gas into the reservoir at pressures above the miscibility pressure in order to improve oil recovery (El-Hoshoudy & Desouky, 2018; Fath & Pournafard, 2014). It is an enhance oil recovery technique. For this case study, CO<sub>2</sub> gas was used for injection. A hybrid model that combines the Todd-Longstaff model, solvent model and miscibility model was used to simulate this process in Eclipse 100 (Schlumberger, 2010). A solvent saturation function and

mixing scale parameter for density and viscosity of fluid and solvent was adopted with a modified PVT table to account for the four phases (Oil, water, gas, and solvent). The miscibility parameter was also set to be dependent on pressure and gas injection fraction to model a realistic case as shown in Figure 4.12. Full miscibility of injected gas starts above 282 bar, which is above the reservoir saturation pressure (258.2 bar).

```

-----
-- DENSITY OF THE SOLVENT
-----
SDENSITY
1.87 /
/

-----
-- MISCIBILITY FUNCTION TABLE
-----
MISC
-- SOL.FRAC  MISC.SCALE
   0.0        0.0
   0.1        0.5
   0.3        1.0
   1.0        1.0
/

-----
-- PRESSURE-DEPENDENT MISCIBILITY
-----
PMISC
-- PRES      MISC.SCALE
   68        0.0
  206        0.3
  282        1.0
  551        1.0
/

-----
-- TODD-LONGSTAFF MMIXING PARAMETER FOR DENSITY AND VISCOSITY
-----
TLMIXPAR
-- VISC      DENS
   0.7      /

```

Figure 4.12. *Some Miscibility Functionalities used for Miscible Flooding (Generated by Eclipse)*

The miscible gas injection scenario was set quite similar to the gas injection case. Four gas injectors (Y2-G, INJ1-G, INJ2-G, and INJ3-G) were retained. In order to re-pressurize the reservoir above miscibility pressure and create a flood front to push the gas, water was injected by four water injector wells (Y2-W, INJ1-W, INJ2-W, and INJ3-W) in and the miscible gas injection scheme was initiated to an economic BHP constrain of 100 bars. The water and gas injection wells were constrained to a maximum surface injection rate of 3000 Sm<sup>3</sup>/d and 100,000 Sm<sup>3</sup>/d with each injector well limited to an injection pressure of 475 bars. Figure 4.13 and Table 4.3 show the positions of the wells.

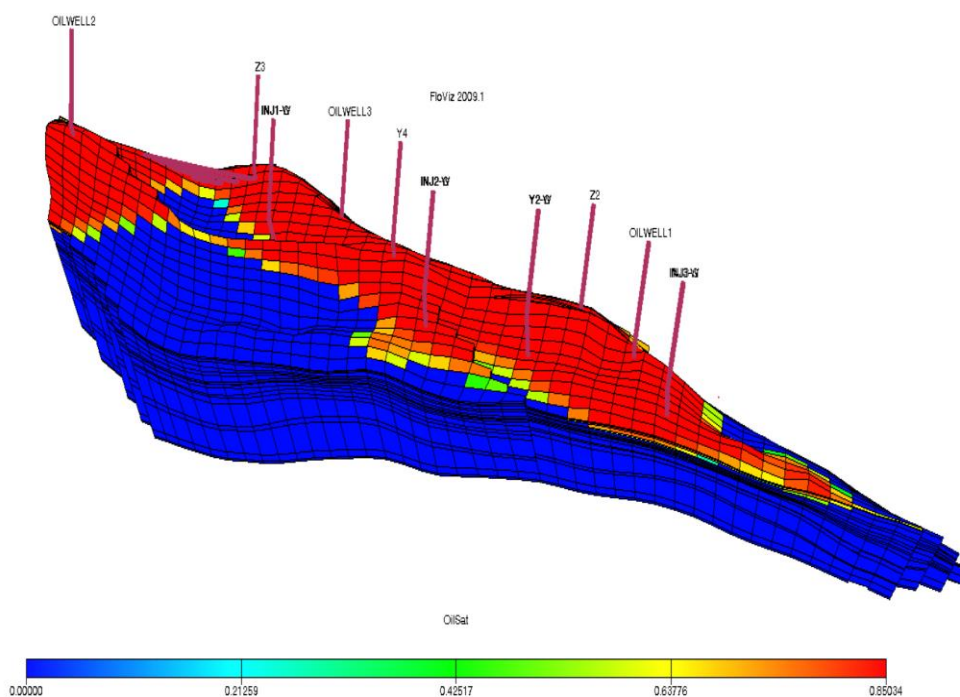


Figure 4.13. Well Position for Miscible Flooding Scenario (Generated by Flviz)

Table 4.3.

*Position and grid geometry of wells for miscible CO<sub>2</sub> injection*

Well	I	J	Phase	Status	Geometry	Rate (Sm <sup>3</sup> /d)
Z2	11	26	Oil	Producer well	Deviated	2400
Z3	20	13	Oil	Producer well	Deviated	2400
Y4	12	21	Oil	Producer well	Vertical	1800
Y2-G	6	28	Gas	Injector well	Vertical	1800
Y2-W	6	28	Water	Injector well	Vertical	3000
OILWELL1	8	33	Oil	Producer well	Vertical	1800
OILWELL2	14	2	Oil	Producer well	Vertical	1800
OILWELL3	17	18	Oil	Producer well	Vertical	1800
INJ1-G	13	15	Gas	Injector well	Vertical	100000
INJ2-G	6	23	Gas	Injector well	Vertical	80000
INJ3-G	3	35	Gas	Injector well	Vertical	100000
INJ1-W	13	15	Water	Injector well	Vertical	3000
INJ2-W	6	23	Water	Injector well	Vertical	3000
INJ3-W	3	35	Water	Injector well	Vertical	3000

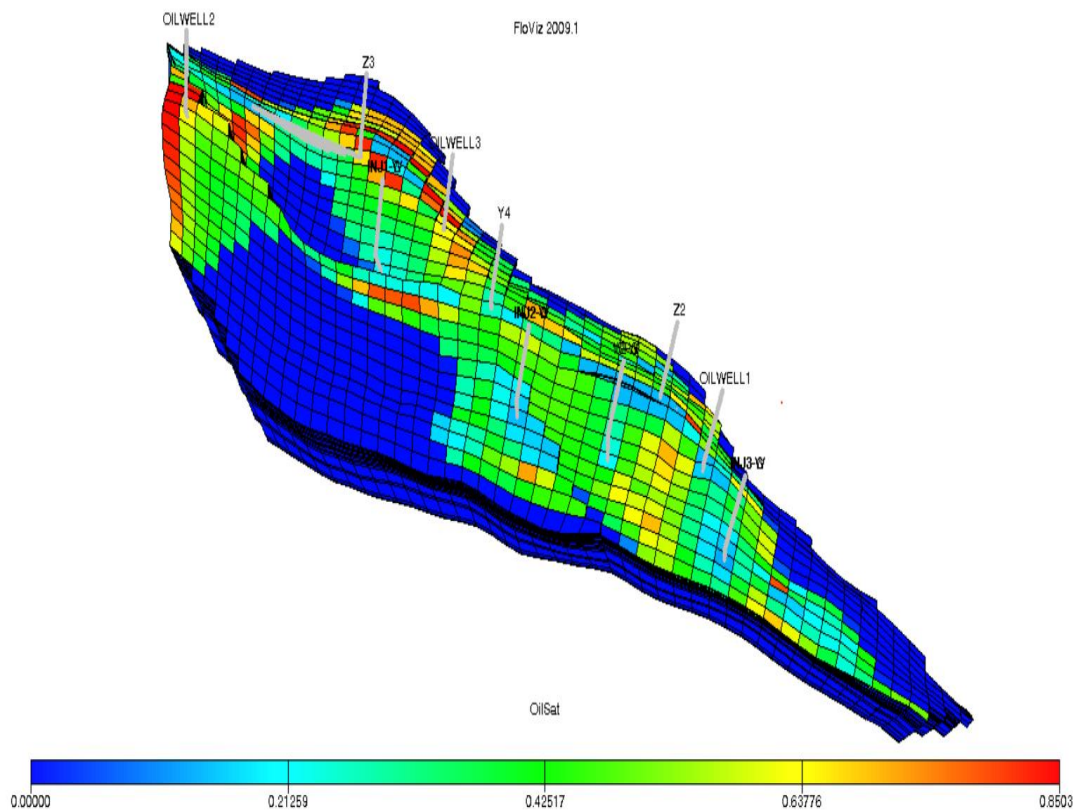


Figure 4.14. *Depletion of Field after Producing with Miscible Flooding (Generated by Flviz)*

Figure 4.14 depletion plot after simulation for a 10-year period. The simulated model consists of four appraisal wells Y4, Y2, Z2, and Z3, and three vertical production wells OILWELL1, OILWELL2, and OILWELL3. Three vertical gas injection wells GASINJ1, GASINJ2 and GASINJ3. Three water injection wells were also drilled (INJ1-W, INJ2-W, and INJ3-W), making a total of 6 production wells and 8 injection wells as well Y2 was converted to a gas injector well, due to excess water production and low oil productivity.

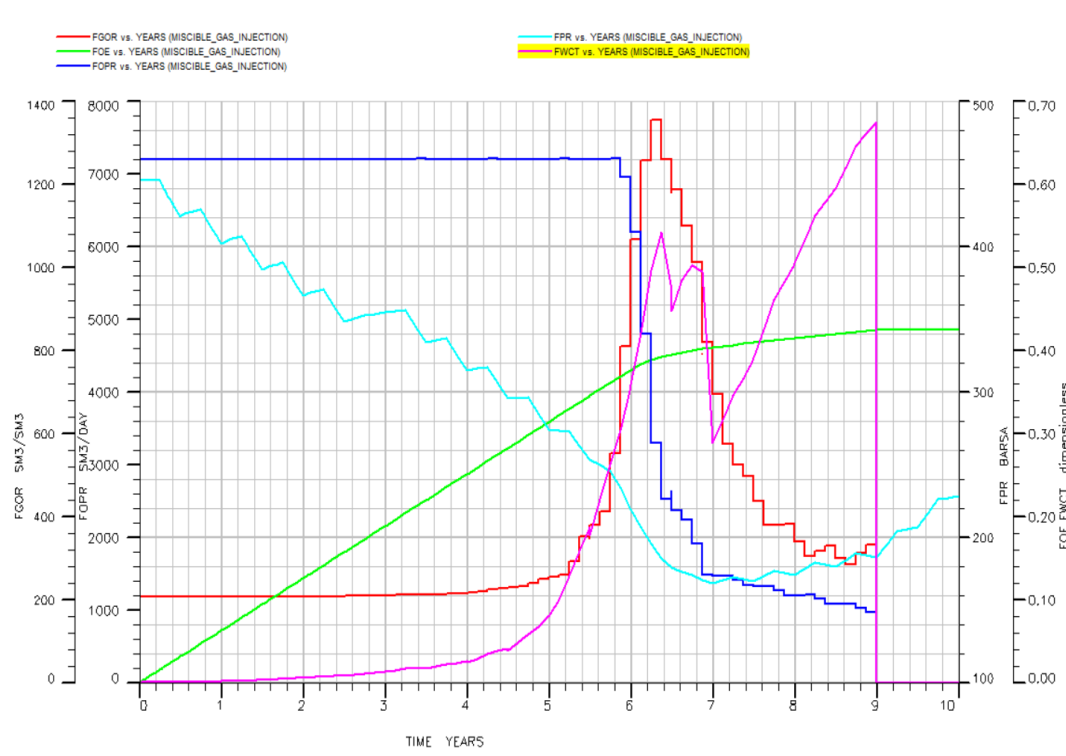


Figure 4.15. Field Performance Plots for Miscible CO<sub>2</sub> Flooding Scenario (Generated by Floviz)

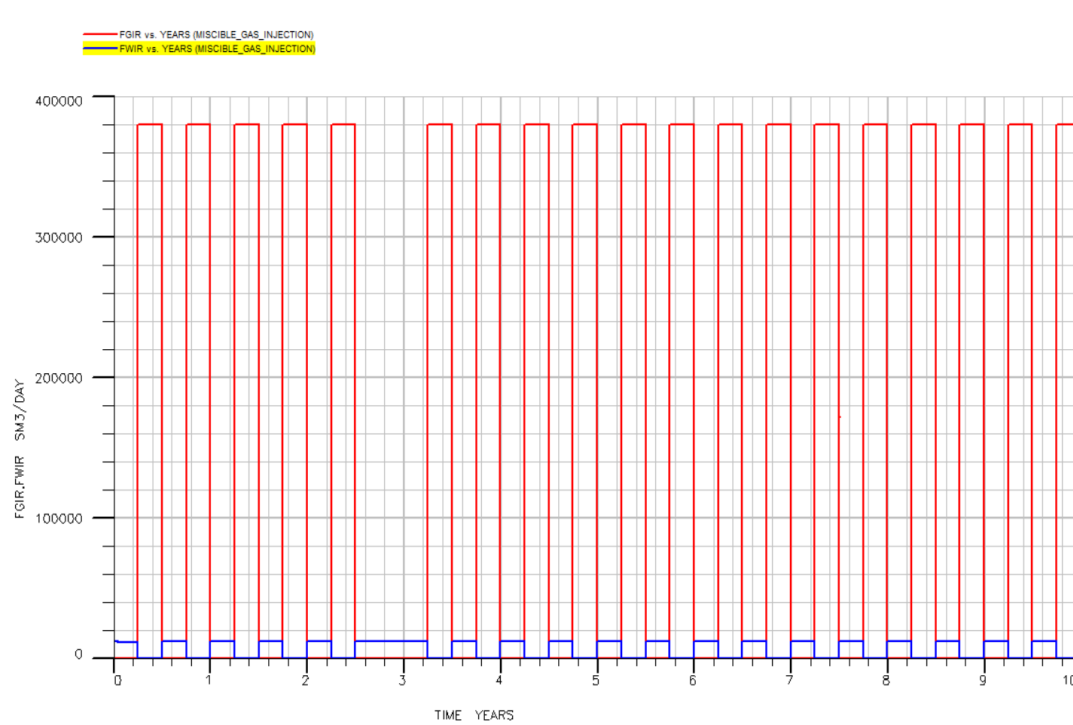


Figure 4.16. Field Injection Plots for Miscible Flooding Scenario (Generated by Floviz)

Figure 4.15 and 4.16 shows the field performance during miscible injection. This is a step wise decline in pressure due to simultaneous gas and water injection. Oil production was sustained for about 9 years before reaching the economic constraint of 1000 Sm<sup>3</sup>/d. FWCT increased up to 68%. Oil recovered by miscible gas injection was 42%. The plateau was maintained for about 5.8 years before declining rapidly. The field produced for about 9 years before shut down.

### Comparative Plots

A comparative plot of the development scenario using natural depletion, immiscible gas injection and miscible gas injection is presented in Figure 4.17 to 4.19.

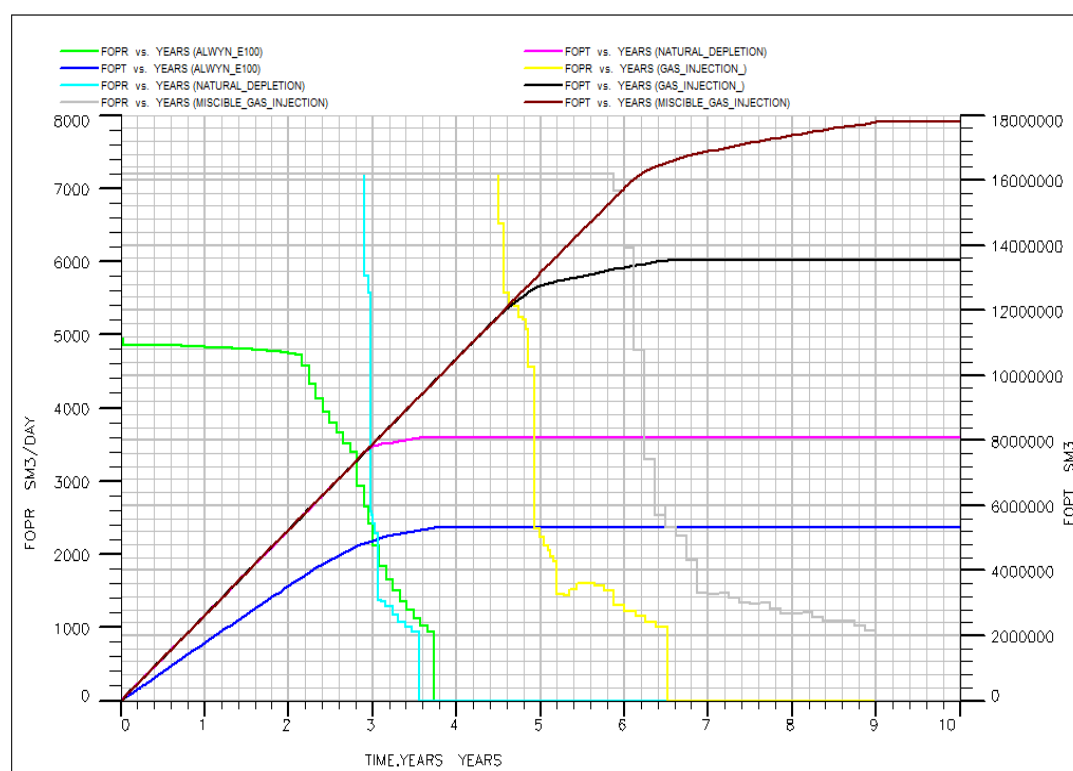


Figure 4.17. Field Oil Production Performance Plots for Initial, Natural Depletion, Immiscible Gas Injection and Miscible Flooding Development Scenario (Generated by Floviz)

Oil recovery was 42%, 30%, 19%, and 13% for miscible injection, immiscible gas injection, and natural depletion cases respectively. Miscible CO<sub>2</sub> injection has the highest oil production total of 17800000 Sm<sup>3</sup>, 13500000 Sm<sup>3</sup> for immiscible gas injection and 8000000 Sm<sup>3</sup> for natural depletion. Therefore, miscible injection shows a better performance compared to other recovery techniques.

Table 4.4.

*Summary of simulation results of natural depletion, immiscible gas injection and miscible CO<sub>2</sub> injection*

S/N	Description	Time (yrs)	FOPT (sm <sup>3</sup> )	FOE (%)	FWCT (%)	FPR (bar)
1	Natural depletion	3.6	8000000	19	67	160
2	Immiscible gas inj.	6.5	13500000	32	56	235
3	Miscible CO <sub>2</sub> inj.	9	17800000	42	68	230

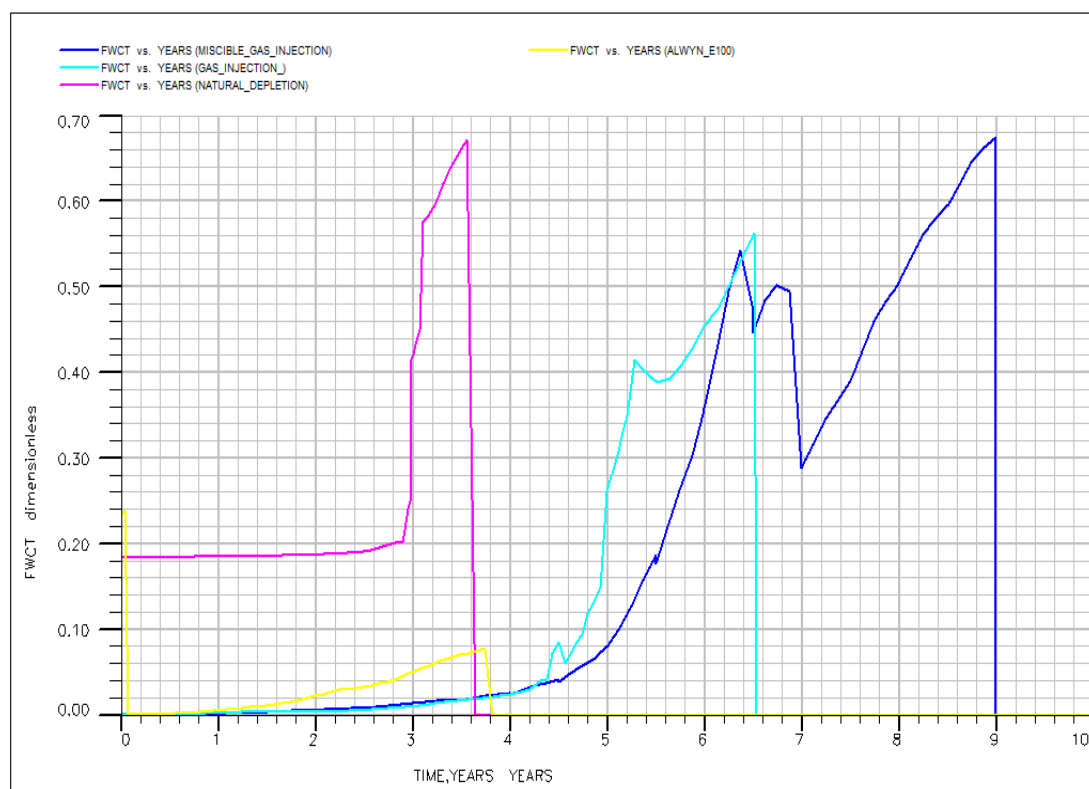


Figure 4.18. *Field Water Cut Plots for Initial, Natural, Gas Injection and Miscible Flooding Development Scenario (Generated by Floviz)*

Field water cut was also compared for all cases. Natural depletion case had early water break through with well Y2 being a major contributor to water produced. Gas injection and miscible gas injection followed same water cut trend.

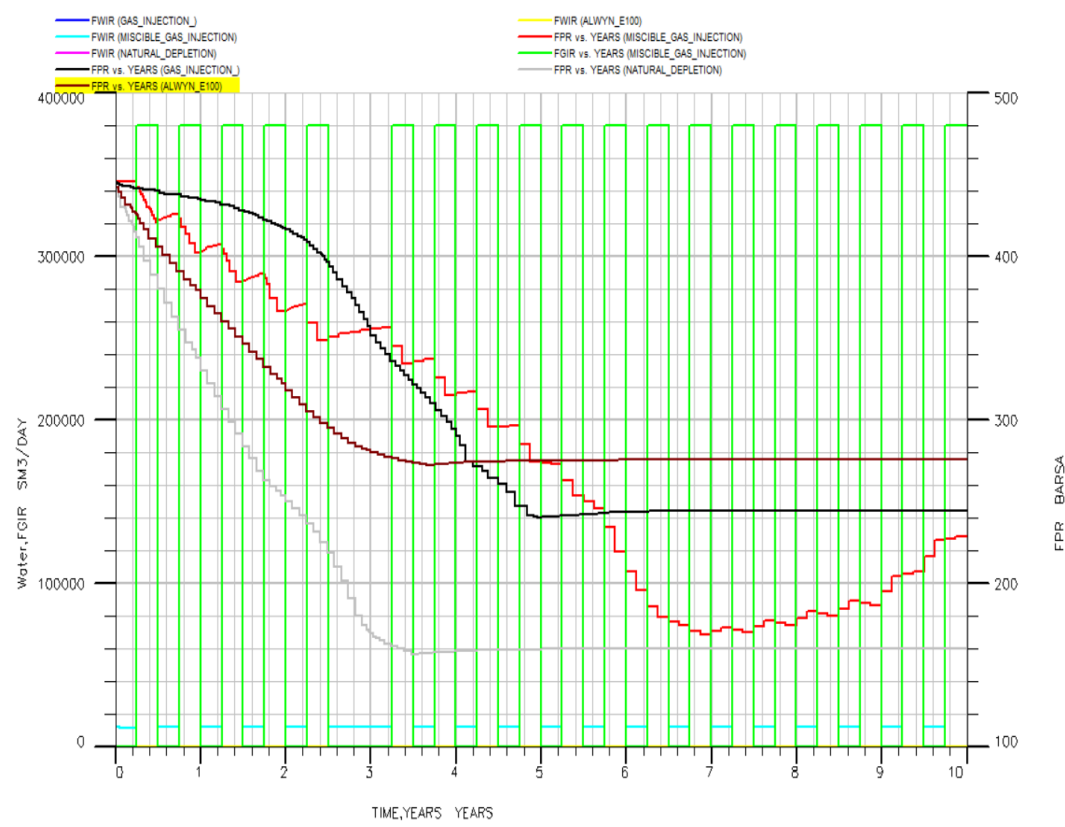


Figure 4.19. *Field Water and Gas Injection in Relation to Field Pressure during Miscible Flooding in Comparison to Field Pressure during Initial, Natural, and Gas Injection (Generated by Floviz)*

The pressure trends for each case are shown in Figure 4.19. The natural case had the most pressure depletion as there was no recharge of the reservoir pressure. Miscible injection had the least pressure decline with time. Pressure declined in a stepwise manner following alternating injection of miscible gas and water. A pressure recharge was noticed from year 7 because the pressure representative of the volume of fluid is withdrawn was less than the pressurization potential of the injected fluid (miscible gas and water). Miscible injection, therefore, shows a better performance than natural depletion and gas injection even when the volumes of gas injected are lower.

### CO<sub>2</sub> Flooding Projects and Case Studies

Due to its availability in adequate quantities from both industrial and natural sources, CO<sub>2</sub> and carbonated water have reportedly been employed to increase oil recovery since 1951 (Abdelaziz & Saad, 2018). The Asmari reservoir, which has two reservoirs and lies southwest of the Iranian oil field, was the subject of research by



Fath & Pouranfard in 2014. With an oil recovery factor of 36.59%, the best miscible CO<sub>2</sub> injection rates were 30,000 Mscf/day (850,000 sm<sup>3</sup>/day) (Fath & Pouranfard, 2014).

In 2014, about 22 businesses engaged in CO<sub>2</sub> flooding. According to Jishun et al. (2015), 126 million tonnes of oil were produced by 128 projects, of which 55 and 37 percent were applied to carbonate and sandstone reservoirs, respectively, and the remaining 6 percent to tripolite reservoirs. With a permeability of 100 mD, the porosity ranges from 4 to 29.5 percent. The key operators and their outcomes are displayed in Table 4.5.

Table 4.5.

*CO<sub>2</sub> miscible flooding operator and production dataset (Abdelaziz & Saad, 2018)*

<b>Operators</b>	<b>No. of projects</b>	<b>Improved prod. (x10<sup>4</sup> tons)</b>	<b>Recovered oil (%)</b>
Occidental	33	459.63	36.37
Kinder Morgan	3	138.34	10.94
Chevron	7	126.30	9.99
Hess	4	106.89	8.46
Denbury Resources	18	86.82	6.87
Merit Energy	7	71.12	5.63
Anadarko	6	55.79	1.94
ExxonMobil	1	36.87	3.59
Breitburn Energy	5	36.87	2.92
ConocoPhillips	2	28.42	2.25
Whiting Petroleum	1	24.51	1.94
Apache	5	23.88	1.89
XTO Energy Inc.	4	13.43	1.06
Chaparral Energy	8	9.18	0.73
Fasken	5	4.30	0.34
Core Energy	9	1.90	0.15
Others	12	31.19	2.47

Table 4.6.

*Reservoir properties under CO<sub>2</sub> flooding dataset (Abdelaziz & Saad, 2018)*

<b>Property</b>	<b>Unit</b>	<b>Minimum</b>	<b>Maximum</b>	<b>Median</b>	<b>Mean</b>
Net thickness	Ft	15	268	90	110
Temperature	F	83	260	108.5	133.9
Porosity	%	4	29.5	12	14.25
Permeability	md	2	700	14	44.35
API gravity	API	27	45	38	37
Oil Saturation	%	26.3	89	46	49.6
Viscosity	cp	0.4	6	1.8	1.3
Depth	ft	1150	11,950	5500	6107.3
Minimum miscible pressure	psia	1020	3452	1987.5	20584

Table 4.5, which details the outcomes of various CO<sub>2</sub> flooding experiments, shows that the recovery factor varied from 0.15% to 36.37%. Table 4.6, summarizes the reservoir characteristics. It can be inferred that majority of the reservoirs had low porosity and permeability with mean of 14.25% and 44.35mD respectively, hence the reason for low recovery factor as seen in Table 4.5. Case one in Table 4.5 with operator Occidental had a close recovery factor (36.37%) to that simulated for this study (42%) because the methodology used in this study was similar to that used by Fath and Pouranfard (2014). Oil recovery discrepancy would be due to porosity and permeability difference and other reservoir and injection parameters (sandstone versus carbonate reservoirs, pressures, and rates).

The Figure 4.20 bellow demonstrates how CO<sub>2</sub> has been used for EOR over time and by various operators in other fields, which satisfies the first and second objectives of this study. However, when compared to the simulation performed on the Alwyn field case study, there is an improved performance in oil recoveries when compared to other studies. However, we may also argue that simulations are accurate representations of reality to a certain extent, mostly used to inform our selection of development approaches. Given the considerable results obtained when CO<sub>2</sub> was utilized, it can be suggested that CO<sub>2</sub> is a reliable EOR technique in modern developments.

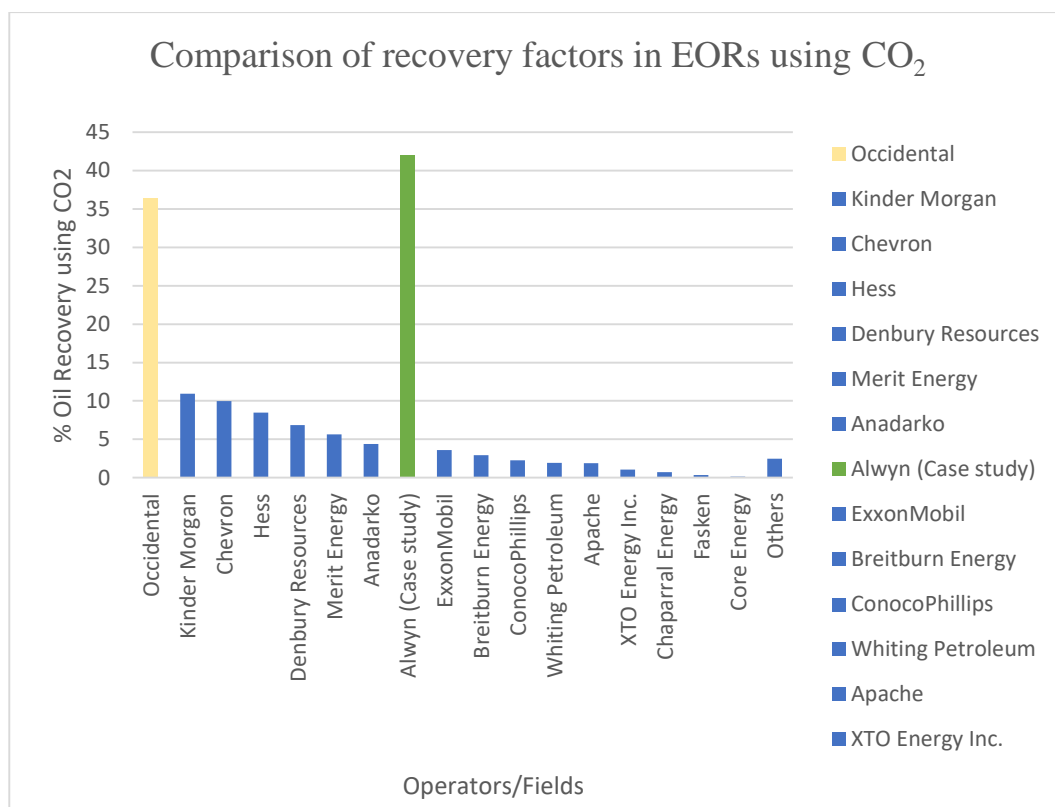


Figure 4.20. Comparison of Oil Recoveries using CO<sub>2</sub> in EORs with Alwyn Case Study (Generated by Excel)

## CHAPTER V

### Conclusions and Recommendations

#### Conclusions

The simulation's goal was to estimate how the Alwyn field would function under miscible gas injection in terms of oil recovery, production rates, and pressure. A model can be built or run numerous times at minimal cost over a short period of time, whereas the field can only be produced once at great expense. To contrast and demonstrate the necessity of miscible gas injection EOR methods, two additional instances were run.

The field produced for 3.6 years under a natural depletion scenario until running out of oil at its economic cap of 1000 Sm<sup>3</sup>/d. Pressure in the reservoir dropped quickly and steadily. This behaviour of the reservoir pressure is related to the lack of extraneous fluids or gas caps that may replace the oil & gas withdrawals. Therefore, it is crucial that we keep the reservoir pressure as high as possible throughout production, preferably above the reservoir fluid's bubble point. Technically, this process is known as pressure maintenance. The maximum FGOR is 1500 Sm<sup>3</sup>/Sm<sup>3</sup> it increased rapidly with a reduction in pressure below the bubble point (258.2 bars), as FWCT increased to 67%.

The gas injection scenario was less water production as field water cut was about 56% after 6 years of production. There was an early gas breakthrough at pressures above saturation pressure, and the gas-oil ratio increased continuously. Compared to natural depletion, oil recovery via gas injection has a significantly higher recovery efficiency. The field was produced for about 6.5 years before shut down. Oil recovery was 32%.

Miscible gas injection had the best production profile and highest oil recovery of about 42%, topping all other simulation scenarios. This is a stepwise decline in pressure due to simultaneous gas and water injection-assisted production. Oil production was sustained for about 9 years before reaching the economic constraint of 1000 sm<sup>3</sup>/d. FWCT increased up to 68%.

The simulation presents a pathway for carbon capture and sequestration prospects in reservoir engineering in addition to detailing the potential for miscible gas injection (CO<sub>2</sub>) as an EOR technique.

## Recommendations

- From the simulation, miscible gas injection is a better recovery technique than natural and gas injection, however the process may be best applied after secondary recovery options have been exhausted.
- Miscible gas (CO<sub>2</sub>) injection also provides a global opportunity for Carbon Capture and Sequestration (CCS). The model can be adopted and improved on to further model this CCS method.
- Although miscible gas injection gave the most oil recovery, it is beneficial to also perform an economic analysis to estimate the cost per barrel and evaluate the profitability of the investment. This can be an area of future research.

## References

- Amadi, A. H., Raphael, O., & Ebube, O. F. (2020). Comparative Analysis of Water Drive, Gas Drive and Natural Drive Mechanism for Oil Production using Alwyn North Field as a Case Study. *European Journal of Engineering and Technology Research*, 5(4), 479–484.  
<https://doi.org/10.24018/ejeng.2020.5.4.1892>
- Beecy, D., & Kuuskraa, V. (2005). Basin Strategies for Linking CO<sub>2</sub> Enhanced Oil Recovery and Storage of CO<sub>2</sub> Emissions. *Greenhouse Gas Control Technologies* 7, 351–359. <https://doi.org/10.1016/b978-008044704-9/50036-7>
- Briggs, J., & Puttagunta, V. (1984). The effect of Carbon dioxide on the Viscosity of Lloydminster Aberfeldy Oil at Reservoir Temperature. *Article Research Council Report Edmonton Alberta*, 110–115.
- Farouq, A. (2016). The Unfulfilled Promise of Enhanced Oil Recovery – More Lies ahead? *Society of Petroleum Engineers*, 244–250.
- El-hoshoudy, A. N., & Desouky, S. (2018). CO<sub>2</sub> Miscible Flooding for Enhanced Oil Recovery. *Carbon Capture, Utilization and Sequestration*.  
<https://doi.org/10.5772/intechopen.79082>
- Philip Chen, C. L., & Zhang, C.-Y. (2014). Data-intensive applications, challenges, techniques and technologies: A survey on big data. *Information Sciences*, 275, 314–347. <https://doi.org/10.1016/j.ins.2014.01.015>
- Chung, F. T. H., Jones, R. A., & Burchfield, T. E. (1988). Recovery of viscous oil under high pressure by CO<sub>2</sub> Displacement: A laboratory study. *International Meeting on Petroleum Engineering*. <https://doi.org/10.2118/17588-ms>
- Conaway, C. F. (1999). The Petroleum Industry: A Nontechnical Guide. *Pennwell Corp; 1st Edition*, 256–274. <https://doi.org/ISBN-13: 978-0878147632>
- DTI SHARP. (2019). ‘CO<sub>2</sub>-EOR Issues Phase 2: Pressure Management and Compositional Effects.’ *ECL Technology*, 108–222.

- DTI SHARP. (2019a). 'CO<sub>2</sub>-EOR Issues: Phase 1 – Literature Review'. *ECL Technology*, 145–296.
- DTI SHARP. (2019b). 'Effect of Impure CO<sub>2</sub> on Miscibility under the UKCS Conditions.' *ECL Technology*, 257–300.
- El-hoshoudy, A. N., & Desouky, S. (2018). CO<sub>2</sub> Miscible Flooding for Enhanced Oil Recovery. *Carbon Capture, Utilization and Sequestration*.  
<https://doi.org/10.5772/intechopen.79082>
- Emera, M. K., & Sarma, H. K. (2006). A Genetic Algorithm-based Model to Predict Co-oil Physical Properties for Dead and Live oil. *Canadian International Petroleum Conference*. <https://doi.org/10.2118/2006-197>
- EPRI (2015). 'Enhanced Oil Recovery Scoping Study', p. TR-113836.
- Espie, A., Brand, P., Skinner, R., Hubbard, R., & Turan, H. (2017). Obstacles to the storage of CO<sub>2</sub> through EOR operations in the North Sea. *Greenhouse Gas Control Technologies - 6th International Conference*, 213–218.  
<https://doi.org/10.1016/b978-008044276-1/50034-9>
- European Commission. (2005). *EUROSTAT Databases*. Retrieved March 3, 2022, from <http://epp.eurostat.cec.eu.int/>
- European Commission. (2017). 'European Energy and Transport, Scenarios on Key Drivers'. Retrieved March 3, 2022.
- European Commission. (2018). 'World Energy, Technology and Climate Policy Outlook 2030'. Retrieved March 3, 2022.
- Hashemi Fath, A., & Pouranfard, A.-R. (2014). Evaluation of Miscible and Immiscible CO<sub>2</sub> Injection in one of the Iranian Oil Fields. *Egyptian Journal of Petroleum*, 23(3), 255–270. <https://doi.org/10.1016/j.ejpe.2014.08.002>
- Goodyear, S. G., Hawkyard, I. R., Masters, J. H. K., Woods, C. L., Jayasekera, A. J., & Balbinski, D. E. (2017). Subsurface issues for CO<sub>2</sub> Flooding of Ukcs Reservoirs. *Chemical Engineering Research and Design*, 81(3), 315–325.  
<https://doi.org/10.1205/02638760360596865>

- Gozalpour, F. (2015). 'CO<sub>2</sub> EOR and Storage in Oil Reservoirs.' *Oil and Gas Science and Technology*, 60(3), 537–546.
- Green, D. W., & Willhite, G. P. (2018). 'Society of Petroleum Engineers, Enhanced Oil Recovery', *In SPE Textbook Series Vol. 6*.
- Holm, L. W., & Josendal, V. A. (2014). Mechanisms of Oil Displacement by Carbon dioxide. *Journal of Petroleum Technology*, 26(12), 1427–1438.  
<https://doi.org/10.2118/4736-pa>
- IEA Greenhouse Gas. (2020). 'Barriers to Overcome in Implementation of CO<sub>2</sub> Capture and Storage (1): Storage in Disused Oil and Gas Fields', p. PH3/22.
- Jayasekera, A. J., & Goodyear, S. G. (2019). Improved Hydrocarbon Recovery in the United Kingdom continental Shelf: Past, Present and Future. *All Days*.  
<https://doi.org/10.2118/75171-ms>
- Jayasekera, T. (2015). Optimisation of CO<sub>2</sub> Injection into UKCS Oilfields. , *In 26th IEA EOR Symposium, Tokyo*.
- Jiang, J., Rui, Z., Hazlett, R., & Lu, J. (2019). An integrated technical-economic model for evaluating CO<sub>2</sub> Enhanced Oil Recovery Development. *Applied Energy*, 247, 190–211. <https://doi.org/10.1016/j.apenergy.2019.04.025>
- Qin, J., Han, H., & Liu, X. (2015). Application and enlightenment of Carbon dioxide flooding in the United States of America. *Petroleum Exploration and Development*, 42(2), 232–240. [https://doi.org/10.1016/s1876-3804\(15\)30010-0](https://doi.org/10.1016/s1876-3804(15)30010-0)
- Kamari, A., Arabloo, M., Shokrollahi, A., Gharagheizi, F., & Mohammadi, A. H. (2015). Rapid method to estimate the Minimum Miscibility Pressure (MMP) in live reservoir oil systems during CO<sub>2</sub> flooding. *Fuel*, 153, 310–319.  
<https://doi.org/10.1016/j.fuel.2015.02.087>
- Kokal, S. L., & Sayegh, S. G. (2019). Phase behavior and physical properties of co-saturated heavy oil and its constitutive fractions. *Annual Technical Meeting*.  
<https://doi.org/10.2118/90-65>



- Kulkarni, M. (2018). Immiscible and miscible gas-oil displacements in porous media. [https://doi.org/10.31390/gradschool\\_theses.259](https://doi.org/10.31390/gradschool_theses.259)
- Lake, L. W., Johns, R., Rossen, B., & Pope, G. (2015). 'Fundamentals of Enhanced Oil Recovery.' *Society of Petroleum Engineers (SPE)*.
- Lake, L. W., Lotfollahi, M., & Bryant, S. L. (2019). CO<sub>2</sub> Enhanced Oil Recovery Experience and its messages for CO<sub>2</sub> Storage. *Science of Carbon Storage in Deep Saline Formations*, 15–31. <https://doi.org/10.1016/b978-0-12-812752-0.00002-2>
- Mahdaviara, M., Nait Amar, M., Hemmati-Sarapardeh, A., Dai, Z., Zhang, C., Xiao, T., & Zhang, X. (2021). Toward Smart Schemes for Modeling CO<sub>2</sub> Solubility in Crude Oil: Application to Carbon dioxide Enhanced Oil Recovery. *Fuel*, 285, 119147. <https://doi.org/10.1016/j.fuel.2020.119147>
- Mehrotra, A. K., & Svrcek, W. Y. (1985). Correlations for Properties of Bitumen saturated with CO<sub>2</sub>, CH<sub>4</sub> and N<sub>2</sub>, and Experiments with Combustion Gas Mixtures. *Journal of Canadian Petroleum Technology*, 21(06). <https://doi.org/10.2118/82-06-05>
- Meyer, J. (2007). Summary of Carbon dioxide Enhanced Oil Recovery (CO<sub>2</sub>EOR) Injection Well Technology. *American Petroleum Institute*. p. 54.
- Miller, J. S., & Jones, R. A. (1981). A laboratory study to determine physical characteristics of heavy oil after CO<sub>2</sub> Saturation. *SPE/DOE Enhanced Oil Recovery Symposium*. <https://doi.org/10.2118/9789-ms>.
- Mulliken, C. A., & Sandler, S. I. (2018). The prediction of CO<sub>2</sub> solubility and swelling factors for enhanced oil recovery. *Industrial & Engineering Chemistry Process Design and Development*, 19(4), 709–711. <https://doi.org/10.1021/i260076a033>
- Rostami, A., Arabloo, M., Lee, M., & Bahadori, A. (2018). Applying SVM framework for Modeling of CO<sub>2</sub> Solubility in Oil during CO<sub>2</sub> flooding. *Fuel*, 214, 73–87. <https://doi.org/10.1016/j.fuel.2017.10.121>

- Peng, D.-Y., & Robinson, D. B. (1976). A new two-constant Equation of State. *Industrial & Engineering Chemistry Fundamentals*, 15(1), 59–64. <https://doi.org/10.1021/i160057a011>
- Perera, M. S. A., Ranjith, P. G., Airey, D. W., & Choi, S. K. (2017). Sub- and super-critical carbon dioxide flow behavior in naturally fractured black coal: An experimental study. *Fuel*, 90(11), 3390–3397. <https://doi.org/10.1016/j.fuel.2011.05.016>
- Peteves, E. T. (2018). Controlling Carbon Emissions: The Option of Carbon Sequest. *European Commission*. (20752 EN).
- Pierce, M., Ranjith, P. G., Airey, D. W., & Choi, S. K. (2017). Drilling and Production, Special Report Enhanced Oil Recovery Survey. *Oil and Gas Journal*.
- Ranathunga, A. S., Perera, M. S., & Ranjith, P. G. (2014). Deep coal seams as a Greener Energy Source: A Review. *Journal of Geophysics and Engineering*, 11(6), 063001. <https://doi.org/10.1088/1742-2132/11/6/063001>
- Rostami, A., Arabloo, M., Kamari, A., & Mohammadi, A. H. (2017). Modeling of CO<sub>2</sub> Solubility in Crude oil during Carbon dioxide Enhanced Oil Recovery using Gene Expression Programming. *Fuel*, 210, 768–782. <https://doi.org/10.1016/j.fuel.2017.08.110>
- Schlumberger, A. (2010). Eclipse Technical Description. *Schlumberger Information Solutions*.
- Schrag, D. P. (2017). Preparing to Capture Carbon. *Science*, 315(5813), 812–813. <https://doi.org/10.1126/science.1137632>.
- Schulte, W. (2014). Experience for Use in CO<sub>2</sub> for Enhanced Oil Recovery in the USA. *In Presentation to the 2014 CO<sub>2</sub> Conference, Norway*.
- SHARP, D. (2017). CO<sub>2</sub> Injection for Heavy Oil Reservoirs. *ECL Technology*.
- Simon, R., & Graue, D. J. (2018). Generalized Correlations for Predicting Solubility, Swelling and Viscosity behavior of CO<sub>2</sub>-Crude Oil Systems.

*Journal of Petroleum Technology*, 17(01), 102–106.

<https://doi.org/10.2118/917-pa>

Srivastava, R., Huang, S., & Dyer, S. (2017). Measurement and Prediction of PVT properties of heavy and medium Oils with Carbon dioxide. *UNITAR New York, NY (United States)*.

Technology, E. (2018). 'CO<sub>2</sub> EOR Issues: Phase I – MMP Calculations.' *DTI SHARP*.

Todd, M. R., & Longstaff, W. J. (1972). The development, testing, and application of a Numerical Simulator for predicting Miscible flood performance. *Journal of Petroleum Technology*, 24(07), 874–882. <https://doi.org/10.2118/3484-pa>

Tunio, S. Q., Tunio, A. H., Ghirano, N. A., & El Adawy, Z. (2011). 'Comparison of different Enhanced Oil Recovery Techniques for better Oil Productivity.' *Int. J. Appl. Sci. Technol.*, (1), pp. 143–153.

Tzimas, E., & Peteves, S. D. (2015). The impact of Carbon Sequestration on the Production Cost of Electricity and Hydrogen from Coal and Natural-Gas Technologies in Europe in the medium term. *Energy*, 30(14), 2672–2689. <https://doi.org/10.1016/j.energy.2004.07.005>

Tzimas, E., Starr, F., & Peteves, D. (2015). The HYPOGEN Project. A *JRC-SETRISration Perspective*, *EUR Report*, (21651 EN).

Verma, M. K. (2015). Fundamentals of Carbon dioxide Enhanced Oil Recovery (CO<sub>2</sub>-EOR): A supporting Document of the Assessment Methodology for Hydrocarbon Recovery using CO<sub>2</sub>-EOR associated with carbon Sequestration. *Open-File Report*. <https://doi.org/10.3133/ofr20151071>

Watson, K., Nelson, E., & Murphy, G. (2018). 'Characterization of Petroleum Fractions.' *Ind Eng Chem*, 27(12), pp. 1460–1480.

Welker, J. R. (2016). Physical Properties of Carbonated Oils. *Journal of Petroleum Technology*, 15(08), 873–876. <https://doi.org/10.2118/567-pa>

Worldometers. (2022). 'World Oil Statistics - Worldometer'. Retrieved April 22, 2022, from <https://www.worldometers.info/oil/>.

Yellig, W. F., & Metcalfe, R. S. (2018). Determination and Prediction of CO<sub>2</sub> Minimum Miscibility Pressures (includes Associated Paper 8876). *Journal of Petroleum Technology*, 32(01), 160–168. <https://doi.org/10.2118/7477-pa>

Zhang, N., Wei, M., & Bai, B. (2018). Statistical and analytical review of worldwide CO<sub>2</sub> Immiscible Field Applications. *Fuel*, 220, 89–100. <https://doi.org/10.1016/j.fuel.2018.01.140>

## Appendices

### Appendix A: Gas Injection PVT File

Maximum Simulation Pressure

PMAX

550 420 1\* 1\* /

/

--- ++++++ WATER ++++++

--- ++++++ W,O,G Gravity ++++++

/

PVTW

-- PRES BW COMPW VISW

446 1.047 5.E-5 0.27 0 /

ROCK

-- PRES COMPR

446 5E-5 /

ECHO

ECHO

-- DENSITY created by PVTi

-- Units: kg /m<sup>3</sup> kg /m<sup>3</sup> kg /m<sup>3</sup>

DENSITY

--

-- Fluid Densities at Surface Conditions

--

829.7675 1020.0000 1.0449

/

-- Column Properties are:

-- 'Oil GOR' 'PSAT' 'Oil FVF' 'Oil Visc'

-- Units: sm3 /sm3 bar rm3 /sm3 cp

PVTO

--

-- Live Oil PVT Properties (Dissolved Gas)

--

0.0000	1.0132	1.0463	3.6674
25.0000	1.0450	3.7326	
50.0000	1.0436	3.7990	
100.0000	1.0411	3.9272	
150.0000	1.0387	4.0495	
175.0000	1.0377	4.1086	
200.0000	1.0366	4.1665	
225.0000	1.0356	4.2231	
250.0000	1.0346	4.2784	
258.2362	1.0343	4.2964	
300.0000	1.0328	4.3858	
350.0000	1.0310	4.4888	
375.0000	1.0302	4.5387	
400.0000	1.0294	4.5877	
409.1537	1.0291	4.6054	
413.7306	1.0290	4.6142	
418.3074	1.0289	4.6230	
450.0000	1.0279	4.6828	
500.0000	1.0265	4.7743	
550.0000	1.0251	4.8625 /	
18.5139	25.0000	1.1266	1.2536
50.0000	1.1213	1.3220	

100.0000	1.1119	1.4561
150.0000	1.1038	1.5868
175.0000	1.1001	1.6509
200.0000	1.0966	1.7142
225.0000	1.0934	1.7767
250.0000	1.0903	1.8384
258.2362	1.0893	1.8585
300.0000	1.0846	1.9595
350.0000	1.0794	2.0775
375.0000	1.0771	2.1355
400.0000	1.0748	2.1927
409.1537	1.0740	2.2135
413.7306	1.0736	2.2238
418.3074	1.0732	2.2341
450.0000	1.0705	2.3050
500.0000	1.0666	2.4145
550.0000	1.0630	2.5213 /
35.3469	50.0000	1.1813
		1.0227
100.0000	1.1695	1.1400
150.0000	1.1595	1.2548
175.0000	1.1550	1.3114
200.0000	1.1507	1.3673
225.0000	1.1468	1.4227
250.0000	1.1430	1.4774
258.2362	1.1418	1.4954
300.0000	1.1362	1.5853
350.0000	1.1300	1.6909
375.0000	1.1271	1.7428
400.0000	1.1244	1.7942
409.1537	1.1235	1.8128
413.7306	1.1230	1.8222
418.3074	1.1225	1.8314
450.0000	1.1193	1.8953
500.0000	1.1147	1.9942

	550.0000	1.1104	2.0910 /
67.7343	100.0000	1.2798	0.7137
	150.0000	1.2651	0.8008
	175.0000	1.2586	0.8439
	200.0000	1.2525	0.8868
	225.0000	1.2469	0.9294
	250.0000	1.2417	0.9718
	258.2362	1.2400	0.9856
	300.0000	1.2321	1.0555
	350.0000	1.2237	1.1381
	375.0000	1.2198	1.1790
	400.0000	1.2161	1.2195
	409.1537	1.2147	1.2343
	413.7306	1.2141	1.2417
	418.3074	1.2135	1.2490
	450.0000	1.2092	1.2997
	500.0000	1.2030	1.3786
	550.0000	1.1973	1.4562 /
103.9068	150.0000	1.3865	0.5143
	175.0000	1.3772	0.5464
	200.0000	1.3686	0.5785
	225.0000	1.3607	0.6105
	250.0000	1.3534	0.6424
	258.2362	1.3511	0.6529
	300.0000	1.3403	0.7060
	350.0000	1.3287	0.7690
	375.0000	1.3235	0.8004
	400.0000	1.3185	0.8316
	409.1537	1.3168	0.8430
	413.7306	1.3159	0.8487
	418.3074	1.3151	0.8543
	450.0000	1.3094	0.8936
	500.0000	1.3012	0.9549
	550.0000	1.2937	1.0156 /



124.0654 175.0000 1.4453 0.4401

200.0000 1.4350 0.4677

225.0000 1.4256 0.4952

250.0000 1.4170 0.5227

258.2362 1.4143 0.5318

300.0000 1.4015 0.5776

350.0000 1.3881 0.6322

375.0000 1.3820 0.6595

400.0000 1.3763 0.6866

409.1537 1.3743 0.6965

413.7306 1.3733 0.7015

418.3074 1.3723 0.7065

450.0000 1.3657 0.7407

500.0000 1.3563 0.7943

550.0000 1.3477 0.8476 /

146.0774 200.0000 1.5092 0.3782

225.0000 1.4980 0.4017

250.0000 1.4877 0.4253

258.2362 1.4845 0.4330

300.0000 1.4695 0.4724

350.0000 1.4538 0.5195

375.0000 1.4467 0.5430

400.0000 1.4400 0.5665

409.1537 1.4376 0.5751

413.7306 1.4365 0.5794

418.3074 1.4354 0.5837

450.0000 1.4278 0.6134

500.0000 1.4169 0.6600

550.0000 1.4071 0.7064 /

170.3161 225.0000 1.5795 0.3260

250.0000 1.5672 0.3461

258.2362 1.5634 0.3527

300.0000 1.5456 0.3864

350.0000 1.5271 0.4267

375.0000	1.5188	0.4469	
400.0000	1.5110	0.4672	
409.1537	1.5083	0.4746	
413.7306	1.5069	0.4783	
418.3074	1.5056	0.4820	
450.0000	1.4968	0.5076	
500.0000	1.4842	0.5479	
550.0000	1.4729	0.5882 /	
197.2831	250.0000	1.6576	0.2819
258.2362	1.6530	0.2875	
300.0000	1.6318	0.3161	
350.0000	1.6099	0.3505	
375.0000	1.6001	0.3678	
400.0000	1.5910	0.3851	
409.1537	1.5878	0.3914	
413.7306	1.5863	0.3946	
418.3074	1.5847	0.3978	
450.0000	1.5745	0.4197	
500.0000	1.5599	0.4544	
550.0000	1.5469	0.4891 /	
206.8974	258.2362	1.6855	0.2688
300.0000	1.6629	0.2959	
350.0000	1.6398	0.3285	
375.0000	1.6294	0.3449	
400.0000	1.6198	0.3613	
409.1537	1.6165	0.3673	
413.7306	1.6148	0.3703	
418.3074	1.6132	0.3733	
450.0000	1.6024	0.3942	
500.0000	1.5871	0.4271	
550.0000	1.5734	0.4601 /	
262.4248	300.0000	1.8468	0.2119
350.0000	1.8154	0.2364	
375.0000	1.8016	0.2488	

400.0000	1.7888	0.2612
409.1537	1.7843	0.2658
413.7306	1.7822	0.2681
418.3074	1.7800	0.2704
450.0000	1.7659	0.2862
500.0000	1.7458	0.3114
550.0000	1.7281	0.3367 /
352.8457	350.0000	2.1123 0.1584
375.0000	2.0917	0.1670
400.0000	2.0728	0.1756
409.1537	2.0663	0.1788
413.7306	2.0631	0.1804
418.3074	2.0599	0.1820
450.0000	2.0393	0.1930
500.0000	2.0105	0.2106
550.0000	1.9853	0.2284 /
418.4723	375.0000	2.3092 0.1347
400.0000	2.2851	0.1417
409.1537	2.2769	0.1443
413.7306	2.2728	0.1456
418.3074	2.2688	0.1468
450.0000	2.2429	0.1558
500.0000	2.2069	0.1701
550.0000	2.1756	0.1846 /
516.4766	400.0000	2.6103 0.1112
409.1537	2.5991	0.1132
413.7306	2.5936	0.1142
418.3074	2.5883	0.1152
450.0000	2.5534	0.1221
500.0000	2.5055	0.1332
550.0000	2.4644	0.1445 /
572.8376	409.1537	2.7881 0.1015
413.7306	2.7817	0.1024
418.3074	2.7755	0.1032

450.0000	2.7351	0.1094
500.0000	2.6798	0.1193
550.0000	2.6326	0.1293 /
611.3386	413.7306	2.9115 0.0959
418.3074	2.9046	0.0968
450.0000	2.8603	0.1025
500.0000	2.7998	0.1116
550.0000	2.7483	0.1209 /
665.6448	418.3074	3.0883 0.0893
450.0000	3.0382	0.0945
500.0000	2.9700	0.1028
550.0000	2.9124	0.1113 /

/

-- Column Properties are:

-- 'Pressure' 'Gas FVF' 'Gas Visc'

-- Units: bar m3 /sm3 cp

PVDG

--

-- Dry Gas PVT Properties (No Vapourised Oil)

--

1.0132	1.3262	0.0109
25.0000	0.0505	0.0126
50.0000	0.0247	0.0136
100.0000	0.0121	0.0153
150.0000	0.0080	0.0175
175.0000	0.0069	0.0189
200.0000	0.0061	0.0203
225.0000	0.0056	0.0217
250.0000	0.0051	0.0232
258.2362	0.0050	0.0237
300.0000	0.0045	0.0261
350.0000	0.0040	0.0289

375.0000	0.0039	0.0302
400.0000	0.00373	0.0314
409.1537	0.00372	0.0319
413.7306	0.00371	0.0321
418.3074	0.0036	0.0324

/

Gas Injection PVT File (Generated from Eclipse100, 2009)

## Appendix B

### Gas Injection Simulation File

-----  
RUNSPEC  
-----

TITLE

BRENT EAST - BO FULL FIELD MODEL WITH E100

DIMENS

36 51 18 /

BLACKOIL

METRIC

DISGAS

GAS

OIL

WATER

TABDIMS

--NTSF NTPV NSSF NPPF NTFP

4 1 25 1\* 1\* /

FAULTDIM

-- NTSEG

24 /

EQLDIMS

-- NTEQUL

3 /

REGDIMS

-- NTFIP NTFIPR

3 18 /

GRIDOPTS

YES /

SATOPTS

'HYSTER' /

WELLDIMS

-- NTW NTCW NTG NTWG NTS NTWS

25 25 4 25 25 10 /

START

1 'JAN' 2022 /

UNIFIN

UNIFOUT

NSTACK

150 /

--NOSIM

-----  
GRID

-----  
RPTGRID

/

GRIDFILE

-- GRD EGRID

0 1 /

-- REQUEST OUTPUT FOR AN INIT FILE

INIT

INCLUDE

'MODEL\_PETREL.GRDECL' /

INCLUDE

'MODEL\_PETREL\_PETRO.GRDECL' /

COPY

PERMX PERMY /

PERMX PERMZ /

/

BOX

1 36 1 51 1 8 /

MULTZ

14688\*0.1 /

ENDBOX

BOX

1 36 1 51 9 12 /

MULTZ

7344\*0.001 /

ENDBOX

BOX

1 36 1 51 13 17 /

MULTZ

9180\*0 /

ENDBOX

PINCH

0.5 /



## MINPV

1000 /

## FAULTS

-- FLT I1 I2 J1 J2 K1 K2 FACE

'FLT1' 8 8 22 23 1 18 X /

'FLT1' 7 8 23 23 1 18 Y /

'FLT1' 6 6 24 24 1 18 X /

'FLT1' 6 6 24 24 1 18 Y /

'FLT1' 5 5 25 25 1 18 X /

'FLT1' 4 5 25 25 1 18 Y /

'FLT1' 3 3 26 26 1 18 X /

'FLT1' 3 3 26 26 1 18 Y /

'FLT1' 2 2 27 27 1 18 X /

'FLT1' 2 2 27 27 1 18 Y /

'FLT1' 1 1 28 28 1 18 X /

'FLT1' 1 1 28 28 1 18 Y /

--

'FLT2' 18 18 1 1 1 18 X /

'FLT2' 18 18 1 1 1 18 Y /

'FLT2' 17 17 2 2 1 18 X /

'FLT2' 16 17 2 2 1 18 Y /

'FLT2' 15 15 3 4 1 18 X /

'FLT2' 15 15 4 4 1 18 Y /

'FLT2' 14 14 5 5 1 18 X /

'FLT2' 14 14 5 5 1 18 Y /

'FLT2' 13 13 6 7 1 18 X /

'FLT2' 13 13 7 7 1 18 Y /

'FLT2' 12 12 8 19 1 18 X /

'FLT2' 12 12 19 19 1 18 Y /

/

## MULTFLT

-- FLT MULT

'FLT1' 0.01 /

'FLT2' 0.00 /

/

-----  
 PROPS  
 -----

INCLUDE

'PVTFUL1.INC' /

PVTW

-- PRES BW COMPW VISW

446 1.047 5.E-5 0.27 0 /

ROCK

-- PRES COMPR

446 5E-5 /

-----  
 -- WATER OIL SATURATION FUNCTIONS  
 -----

SWOF

-- ROCK TYPE 1 = TARBERT

-- SW KRW KRO PCWO

0.150 0.000 0.800 0.600

0.257 0.008 0.481 0.300

0.328 0.015 0.319 0.170

0.400 0.026 0.195 0.095

0.465 0.034 0.123 0.052

0.536 0.050 0.062 0.031

0.602 0.076 0.025 0.018

0.673 0.116 0.010 0.012

0.738 0.186 0.005 0.008

0.780 0.250 0.000 0.001

1.000 1.000 0.000 0.000

/

-- SW KRW KRO PCWO

0.150 0.000 0.800 0.600

0.257 0.008 0.481 0.300

0.328 0.015 0.319 0.170

0.400 0.026 0.195 0.0

0.465 0.034 0.123 -0.05

0.536 0.050 0.062 -0.06

0.602 0.076 0.025 -0.08

0.673 0.116 0.010 -0.2

0.738 0.186 0.005 -0.6

0.780 0.250 0.000 -1.0

/

-- ROCK TYPE 2 = NESS & LOWER BRENT

-- SW KRW KROW PCWO

0.300 0.000 0.800 0.600

0.368 0.008 0.481 0.300

0.413 0.015 0.319 0.170

0.458 0.026 0.195 0.095

0.500 0.034 0.123 0.052

0.545 0.050 0.062 0.031

0.587 0.076 0.025 0.018

0.632 0.116 0.010 0.012

0.674 0.186 0.005 0.008

0.700 0.250 0.000 0.001

1.000 1.000 0.000 0.000

/

-- SW KRW KROW PCWO

0.300 0.000 0.800 0.600

0.368 0.008 0.481 0.300

0.413 0.015 0.319 0.170

0.458	0.026	0.195	0.0
0.500	0.034	0.123	-0.02
0.545	0.050	0.062	-0.03
0.587	0.076	0.025	-0.08
0.632	0.116	0.010	-0.25
0.674	0.186	0.005	-0.64
0.700	0.250	0.000	-1.0

/

-----  
 -- GAS OIL SATURATION FUNCTIONS  
 -----

## SGOF

-- ROCK TYPE 1 = TARBERT

-- SG    KRG    KROG    PCGO

0.000	0.000	0.800	0.000
0.100	0.029	0.551	0.000
0.170	0.070	0.411	0.001
0.240	0.124	0.292	0.002
0.300	0.185	0.200	0.004
0.370	0.261	0.120	0.010
0.430	0.341	0.064	0.019
0.500	0.437	0.023	0.034
0.560	0.534	0.003	0.060
0.700	0.600	0.000	0.120

/

-- SG    KRG    KROG    PCGO

0.000	0.000	0.800	0.000
0.170	0.000	0.411	0.001
0.240	0.030	0.292	0.002
0.300	0.075	0.200	0.004
0.370	0.120	0.120	0.010
0.430	0.180	0.064	0.019
0.500	0.289	0.023	0.034

0.560 0.400 0.003 0.060  
 0.700 0.600 0.000 0.120

/

-- ROCK TYPE 2 = NESS &amp; LOWER BRENT

-- SG KRG KROG PCWO

0.000 0.000 0.800 0.000  
 0.085 0.029 0.551 0.000  
 0.142 0.070 0.411 0.001  
 0.198 0.124 0.292 0.002  
 0.250 0.185 0.200 0.004  
 0.307 0.261 0.120 0.010  
 0.358 0.341 0.064 0.019  
 0.415 0.437 0.023 0.034  
 0.467 0.534 0.003 0.060  
 0.500 0.600 0.000 0.120

/

-- SG KRG KROG PCWO

0.000 0.000 0.800 0.000  
 0.170 0.000 0.411 0.001  
 0.210 0.030 0.292 0.002  
 0.250 0.056 0.200 0.004  
 0.307 0.100 0.120 0.010  
 0.358 0.170 0.064 0.019  
 0.415 0.300 0.023 0.034  
 0.467 0.450 0.003 0.060  
 0.500 0.600 0.000 0.120

/

-----  
 REGIONS

-----  
 SATNUM

1836\*1 1836\*1 1836\*1 1836\*1 1836\*1 1836\*1 1836\*1 1836\*1 1836\*1

1836\*3 1836\*3 1836\*3 1836\*3 1836\*3 1836\*3 1836\*3 1836\*3 1836\*3

/

-- ebubeorisa@yahoo.com

IMBNUM

1836\*2 1836\*2 1836\*2 1836\*2 1836\*2 1836\*2 1836\*2 1836\*2 1836\*2

1836\*4 1836\*4 1836\*4 1836\*4 1836\*4 1836\*4 1836\*4 1836\*4 1836\*4

/

FIPNUM

1836\*1 1836\*1 1836\*1 1836\*1 1836\*1 1836\*1 1836\*1 1836\*1 1836\*1

1836\*2 1836\*2 1836\*2 1836\*2 1836\*2 1836\*2 1836\*2 1836\*2 1836\*2

/

--Equilibrium Regions

--Region 1

BOX

1 36 1 51 1 18 /

EQLNUM

33048\*1 /

ENDBOX

--Region 2

BOX

1 18 1 1 1 18 /

EQLNUM

324\*2 /

BOX

1 17 2 2 1 18 /

EQLNUM

306\*2 /

BOX

1 15 3 4 1 18 /

EQLNUM

540\*2 /

BOX

1 14 5 5 1 18 /

EQLNUM

252\*2 /

BOX

1 13 6 7 1 18 /

EQLNUM

468\*2 /

BOX

1 12 8 11 1 18 /

EQLNUM

864\*2 /

ENDBOX

--Region 3

BOX

1 36 1 51 17 18 /

EQLNUM

3672\*3 /

ENDBOX

RPTREGS

/

-----  
SOLUTION

-----  
EQUIL

-- DATUM PDAT WOC PCWC GOC PCGC PBVD RVVD

-- MET BARS MET BARS MET BARS

3200 446.0 3231 0 500 0 1 0 0 /

3200 446.0 3231 0 500 0 1 0 0 /

3200 446.0 3231 0 500 0 1 0 0 /

PBVD

3100 258

3231 258 /

3100 258

3231 258 /

3100 258

3231 258 /

RPTRST

'BASIC=2' /

RPTSOL

'PRES' 'SOIL' 'SWAT' 'SGAS' 'RESTART=2' 'FIP=3' 'EQUIL' /

-----

SUMMARY

-----

FPR

FBHP

-- FIELD CUMULATIVE PRODUCTIONS & INJECTIONS (IN STOCK  
CONDITONS)

FOPT

FOE

FGPT

FWPT

FWIT

-- FIELD PRODUCTION RATES (IN STOCK CONDITONS)



FOPR

FGOR

FGPR

FWPR

FWCT

FWIR

FGIR

GOPR

GGPR

GWPR

GWCT

GGIR

GGOR

-- FLUIDS IN PLACE (IN STOCK CONDITONS)

FOIP

FGIP

FWIP

-- FLUIDS IN PLACE & (IN RESERVOIR CONDITONS)

FRPV

FOPV

FWPV

FGPV

FPR

-- MATERIAL BALANCE ANALYSIS

FORFR

FORFE

FORFW

FORFS

FORFG

FORMR  
FORME  
FORMW  
FORMS

WOPT

/

WGPT

/

WWPT

/

WWPR

/

WBHP

/

WBP

/

WLPR

/

WOPR

/

WGPR

/

WWPR

/

WWIT

/

WWIT

/

WWIR

/

WGIR

/

WGOR

/

WWCT

/

-----  
 SCHEDULE  
 -----

RPTSCHED

'FIP=3' 'WELLS=2' 'RESTART=2' /

RPTRST

-- RESTART OUTPUT CONTROL

BASIC=2 /

VFPCHK

1E-10 /

TUNING

1 50 /

/

2\* 50/

-- fichier SCH

WELSPECS

-- WELL	GROUP	I	J	DEPTH	PHASE		
'Z2'	'G1'	11	26	3231.0	'OIL'	3*	NO /
'Z3'	'G1'	20	13	2951.5	'OIL'	3*	NO /
'Y2'	'G1'	6	28	3277.6	'GAS'	3*	NO /
'Y4'	'G1'	12	21	3074.0	'OIL'	3*	NO /
'GASINJ1'	'G1'	13	15	3074.0	'GAS'	3*	NO /
'GASINJ2'	'G1'	6	23	3227.6	'GAS'	3*	NO /
'GASINJ3'	'G1'	3	35	3074.0	'GAS'	3*	NO /

'OILWELL1' 'G1' 8 33 3277.6 'OIL' 3\* NO /  
'OILWELL2' 'G1' 14 2 3277.6 'OIL' 3\* NO /  
'OILWELL3' 'G1' 17 18 3277.6 'OIL' 3\* NO /

/

## COMPDAT

-- WELL	I	J	K1	K2	STATUS	KR	TR	DIAM	KH	SKIN
'Z2'	11	26	4	4	'OPEN'	1*	1*	0.216	1*	0./
'Z2'	11	27	4	4	'OPEN'	1*	1*	0.216	1*	0./
'Z2'	11	28	4	4	'OPEN'	1*	1*	0.216	1*	0./
'Z2'	11	29	4	4	'OPEN'	1*	1*	0.216	1*	0./
'Z2'	11	30	4	4	'OPEN'	1*	1*	0.216	1*	0./
'Z2'	11	31	4	4	'OPEN'	1*	1*	0.216	1*	0./
'Z2'	11	32	4	4	'OPEN'	1*	1*	0.216	1*	0./

-- ebubeorisa@yahoo.com

'Z3'	20	13	2	2	'OPEN'	1*	1*	0.216	1*	0./
'Z3'	20	12	2	2	'OPEN'	1*	1*	0.216	1*	0./
'Z3'	20	11	2	2	'OPEN'	1*	1*	0.216	1*	0./
'Z3'	20	10	2	2	'OPEN'	1*	1*	0.216	1*	0./
'Z3'	20	9	2	2	'OPEN'	1*	1*	0.216	1*	0./
'Z3'	20	8	2	2	'OPEN'	1*	1*	0.216	1*	0./
'Z3'	20	7	2	2	'OPEN'	1*	1*	0.216	1*	0./
'Z3'	20	6	2	2	'OPEN'	1*	1*	0.216	1*	0./

'Y2'	6	28	5	14	'OPEN'	1*	1*	0.216	1*	-4/
'Y4'	12	21	2	3	'OPEN'	1*	1*	0.216	1*	0/
'GASINJ1'	13	15	5	7	'OPEN'	1*	1*	0.216	1*	-4/
'GASINJ2'	6	23	3	6	'OPEN'	1*	1*	0.216	1*	-4/
'GASINJ3'	3	35	3	6	'OPEN'	1*	1*	0.216	1*	-4/
'OILWELL1'	8	33	2	7	'OPEN'	1*	1*	0.216	1*	0./

'OILWELL3' 17 18 2 7 'OPEN' 1\* 1\* 0.216 1\* 0. /  
'OILWELL2' 14 2 2 7 'OPEN' 1\* 1\* 0.216 1\* 0. /  
/

## GRUPTREE

'G1' 'FIELD' /  
/

## WCONPROD

'Z2' 'OPEN' 'ORAT' 2400 2\* 2400 1\* 100 /  
'Z3' 'OPEN' 'ORAT' 2400 2\* 2400 1\* 100 /  
--'Y2' 'OPEN' 'ORAT' 1800 2\* 1800 1\* 100 /  
'Y4' 'OPEN' 'ORAT' 1500 2\* 1800 1\* 100 /  
'OILWELL1' 'OPEN' 'ORAT' 1800 2\* 1800 1\* 100 /  
'OILWELL2' 'OPEN' 'ORAT' 1800 2\* 1800 1\* 100 /  
'OILWELL3' 'OPEN' 'ORAT' 1800 2\* 1800 1\* 100 /  
/

## WECON

'Z2' 100 1\* 0.9 1500 1\* +CON/  
'Z3' 100 1\* 0.9 1500 1\* +CON/  
--'Y2' 100 1\* 0.9 1500 1\* +CON/  
'Y4' 100 1\* 0.9 1500 1\* +CON/  
'OILWELL1' 100 1\* 0.9 1500 1\* +CON/  
'OILWELL2' 100 1\* 0.9 1500 1\* +CON/  
'OILWELL3' 100 1\* 0.9 1500 1\* +CON/  
/

-- PRODUCTION RATE CONTROL FOR PRODUCERS GROUP

## GCONPROD

'G1' 'ORAT' 7200 /

/

-- SET A MINIMUM ECONOMIC OIL PRODUCTION

GECON

'G1' 1000 1\* 0.9 1500 1\* WELL/

/

WEFAC

'Z2' 0.9 /

'Z3' 0.9 /

--'Y2' 0.9 /

'Y4' 0.9 /

'OILWELL1' 0.9 /

'OILWELL2' 0.9 /

'OILWELL3' 0.9 /

/

WDRILTIM

-- name	drilling time	well	close	while	drilling
compartment number					

'GASINJ1\*' 60 YES /

'GASINJ2\*' 60 YES /

'GASINJ3\*' 120 YES /

/

WCONINJE

'Y2' GAS 1\* 'GRUP' 800000 1\* 475 /

'GASINJ1' GAS 1\* 'GRUP' 800000 1\* 475 /

'GASINJ2' GAS 1\* 'GRUP' 800000 1\* 475 /

'GASINJ3' GAS 1\* 'GRUP' 800000 1\* 475 /

/

GCONINJE

'G1' 'GAS' 'VREP' 3200000 2\* 1 /  
/

DATES

1 'JAN' 2023 /  
1 'JAN' 2024 /  
1 'JAN' 2025 /  
1 'JAN' 2026 /  
1 'JAN' 2027 /  
1 'JAN' 2028 /  
1 'JAN' 2029 /  
1 'JAN' 2030 /  
1 'JAN' 2031 /  
1 'JAN' 2032 /

/

-- END OF SIMULATION

END

Gas Injection Simulation File (Generated from Eclipse100, 2009)

## Appendix C

### Turnitin Similarity Report

Carvi Atalar | User Info | Messages (1 new) | Instructor | English | Community | Help | Logout

[Assignments](#) | [Students](#) | [Grade Book](#) | [Libraries](#) | [Calendar](#) | [Discussion](#) | [Preferences](#)

NOW VIEWING: HOME > MASTER > OLISA LEONARD OSIMIRI

**About this page**  
 This is your assignment inbox. To view a paper, select the paper's title. To view a Similarity Report, select the paper's Similarity Report icon in the similarity column. A ghosted icon indicates that the Similarity Report has not yet been generated.

**Olisa Leonard Osimiri**  
 INBOX | NOW VIEWING: NEW PAPERS ▾

Submit File

	AUTHOR	TITLE	SIMILARITY	GRADE	RESPONSE	FILE	PAPER ID	DATE
<input type="checkbox"/>	Olisa Leonard Osimiri...	ABSTRACT	0%	--	--		1865387128	01-Jul-2022
<input type="checkbox"/>	Olisa Leonard Osimiri...	CONCLUSION	0%	--	--		1865387145	01-Jul-2022
<input type="checkbox"/>	Olisa Leonard Osimiri...	CHAPTER 2	3%	--	--		1865386821	01-Jul-2022
<input type="checkbox"/>	Olisa Leonard Osimiri...	CHAPTER 4	3%	--	--		1865386873	01-Jul-2022
<input type="checkbox"/>	Olisa Leonard Osimiri...	CHAPTER 1	4%	--	--		1865386812	01-Jul-2022
<input type="checkbox"/>	Olisa Leonard Osimiri...	THESIS	4%	--	--		1865387122	01-Jul-2022
<input type="checkbox"/>	Olisa Leonard Osimiri...	CHAPTER 3	13%	--	--		1865386829	01-Jul-2022

Online Grading Report | Edit assignment settings | Email non-submitters

Copyright © 1999 – 2022 Turnitin, LLC. All rights reserved. | EU Data Protection Compliance | Copyright Protection | Legal FAQs | Helpdesk | Research Resources



## Appendix D

### Ethical Approval Letter



**YAKIN DOĞU ÜNİVERSİTESİ**  
**ETHICAL APPROVAL DOCUMENT**

Date: 29/06/2022

To the **Institute of Graduate Studies**

The research project titled “**NUMERICAL SIMULATION OF MISCIBLE CO<sub>2</sub> INJECTION FOR EOR IN THE ALWYN FIELD, NORTH SEA, UK.**” has been evaluated. Since the researcher will not collect primary data from humans, animals, plants or earth, this project does not need through the ethics committee.

**Title:** Prof. Dr.

**Name Surname:** Cavit ATALAR

**Signature:**

**Role in the Research Project:** Supervisor